UCLA
COMPUTATIONAL AND APPLIED MATHEMATICS

On the Formation of an Interface Singularity in the Rising 2-D Boussinesq Bubble

David A. Pugh
Stephen J. Cowley

November 1992
CAM Report 92-45

Department of Mathematics
University of California, Los Angeles
Los Angeles, CA. 90024-1555

On the formation of an interface singularity in the rising 2-D Boussinesq bubble

David A. Pugh
Mathematics Department,
UCLA, Los Angeles
CA 90024-1555, USA

Stephen J. Cowley
DAMTP, University of Cambridge
Silver Street, Cambridge CB3 9EW, UK

November 3, 1992

Abstract

The evolution of the vortex sheet created at the interface of a two-dimensional cylindrical bubble of light fluid in an infinite volume of heavy fluid is followed using the point-vortex method. Both fluids are assumed to be inviscid and incompressible, surface tension is ignored at the interface, and the flow is taken to be irrotational. A Boussinesq approximation is made.

The evolution equations are integrated forward in time. The filtering technique of Krasny (1986) is used to control the effects of rounding error. It is shown that after a finite time two singularities develop. At the singularity points the curvature of the interface becomes infinite, while the vortex-sheet strength develops a cusp. By means of an asymptotic analysis of the Fourier series of the sheet position, estimates of both the time at which the singularities form, and the singularity structure, are obtained. In particular, it is shown that when the singularity forms the algebraic decay of the Fourier coefficients is proportional to $k^{-2.5}$ where k is the wavenumber.

1 Introduction

One of the simplest models for the motion of a bubble of light fluid through a heavier fluid consists of assuming that both fluids are incompressible and inviscid, and that there is no surface tension at the interface. The buoyancy force arising from the density difference causes the bubble to move upwards.

Due to the differential flow on either side of the fluid interface, a vortex sheet usually develops there, i.e. while the normal velocity is continuous across the interface, the tangential velocity is usually discontinuous. The magnitude of the discontinuity is referred to as the strength of the vortex sheet. In this paper we will study a model problem in which a circular two–dimensional bubble of radius a is instantaneously introduced into the fluid at $t = 0$. We show that after a finite time, singularities develop in the shape of the interface. At the singular points the curvature becomes infinite, while the sheet strength develops a cusp. The singularities occur when the bubble is kidney shaped. They appear on the lower surface of the bubble where the sheet is continually being compressed.

The appearance of a singularity in a vortex sheet was first shown analytically by Moore (1979). He considered small sinusoidal disturbances to a uniform vortex sheet. His results have been confirmed numerically by Meiron, Baker and Orszag (1982), Krasny (1986) and Shelley (1992) (see also Higdon and Pozrikidis, 1985). Using similar methods Rottman, Simpson and Stansby (1987) and Rottman & Stansby (1992) have studied the two–dimensional inviscid motion of an initially circular vortex sheet released from rest in a cross–flow; they also find that singularities develop in the shape of the vortex sheet.

Pugh (1989) has studied flows driven by small (Boussinesq) density differences. He found that as a result of the vortex sheets generated at the density interface, singularities developed in the shape of the interface for such diverse flows as the rise of two–dimensional and axisymmetric bubbles, Rayleigh–Taylor instability, and the descent of a vortex pair towards a stable interface. This is in agreement with Moore's (1981) suggestion that singularities can develop in all vortex sheets that are not being stretched sufficiently rapidly. Siegel (1989) has generalised this work to order one density differences. He argues analytically that in the case of Rayleigh–Taylor instability, singularities can form at the interface between two fluids of different, non-zero, density. Baker, Caflisch & Siegel (1991, private communication) have confirmed this result numerically.

The underlying reason why singularities arise is related to the fact that the the growth-rate of small wavelength disturbances is directly proportional to the wavenumber. As a result small changes in the initial conditions can produce significant changes in the solution at later times; the mathematical problem is said to be ill-posed. Despite this ill–posedness, Sulem *et al.* (1981) proved a short time existence result for analytic initial data, while Caflisch & Orellana (1986) proved existence almost up to the time of singularity formation for initial data close to that of a flat sheet. Caflisch & Orellana (1989) have constructed exact solutions which display singularity formation in physical space; however these solutions, which are almost linear to leading order, are restrictive in that they correspond to special choices of initial conditions.

An important consequence of the ill–posedness is that in numerical calculations perturbations created by machine round-off error are amplified by Kelvin-Helmholtz instability; this can lead to inaccurate solutions. However Krasny (1986) showed for a fixed number of modes (or points), sufficiently high arithmetic precision enabled a smooth regular solution to be obtained until the (possible) development of a singularity. In contrast, he showed that for a given precision a sufficiently large number of modes gave rise to irregular motion of the interface. In order to obtain accurate numerical solutions which are not contaminated by rounding error, Krasny (1986) adopted the following method. At each time step, the discrete Fourier series of the solution is found. Then any modes of magnitude smaller than a given filter level (dependent on the machine precision) are set to zero and the new Fourier series inverted to give the filtered solution. In this way round–off error can be controlled without seriously affecting the non-linear growth of the modes; this is in contrast to methods like linear smoothing and repositioning (e.g. see Moore (1981), Rottman *et al.* (1987)). Furthermore, Krasny (1986) demonstrated that the solution obtained was accurate and converged as the number of Fourier modes, N, increased and the time step, dt, decreased.

In the case of flows involving fluids of two densities, a key parameter governing the motion of the bubble is the Atwood ratio A, defined by

$$A = \frac{\rho_+ - \rho_-}{\rho_+ + \rho_-},$$

where ρ_- and ρ_+ are the densities of the lighter and heavier fluids respectively. The rise of a vacuous bubble in an infinite fluid, corresponding to the case $A = 1$, has been studied by Baumel *et al.* (1982) and Baker and Moore (1989). They found that no singularity developed in the interface shape; indeed Baker and Moore (1989) were able to follow the solution almost up to the moment that the interface intersects itself. We will consider the other extreme case, i.e. the Boussinesq limit in which $A \to 0$ and $g \to \infty$ such that $G = Ag$ remains finite; the parameter G is the modified gravity. The Boussinesq limit is used to model situations in which the two fluids are of almost equal density, and gravity is much greater in magnitude than any acceleration of the vortex sheet. Such situations can arise in geophysical fluid dynamics where a pocket of warm air rises in a slightly cooler atmosphere. For instance, Scorer (1958) suggested that plumes of chimney smoke which are bent horizontal by a crosswind can be described in terms of a two-dimensional buoyancy source.

Similar problems involving the Boussinesq limit have been studied by Hill (1975) in the case of a trailing vortex pair in a stably stratified atmosphere, and by Meng & Thompson (1979) and Rambaldi & Randall (1981) in their studies of rising nascent thermals. Both latter pairs of authors modelled the rising two–dimensional Boussinesq bubble which is the subject of our study. Meng & Thompson (1979) used a vortex blob method, while Rambaldi & Randall (1981) adopted the vortex sheet method used here. However, as shown below, both pairs of authors integrated beyond the time at which a singularity forms in the interface shape; the validity of their solutions is questionable after this time.

Anderson (1985) also studied the evolution of a two–dimensional Boussinesq bubble. He used a vortex blob method due to Chorin and Bernard (1973). In this method a point vortex is replaced by a 'patch of vorticity' of finite radius $\hat{\delta}$ (although the physical significance of this approximation is, as yet, unclear). The equations of motion were modified by a term proportional to the parameter $\hat{\delta}$, and the computations performed for decreasing values of $\hat{\delta}$. Convergence was demonstrated as $\hat{\delta} \to 0$. Anderson (1985) conjectured that interface singularities form in which the arclength tends to infinity. An approximate time of formation was also given but no further conclusions were drawn as to the structure of the singularity.

The motivation for studying the rising bubble arose out of difficulties encountered in studying the motion of an infinite, *non-periodic* vortex sheet in which smoothing and repositioning techniques were used (Pugh, 1989). In particular it was difficult to ascertain whether or not a singularity formed. The two–dimensional Boussinesq bubble, being periodic and therefore amenable to a Fourier series representation and Krasny's (1986) filtering technique, was therefore chosen as an easier model problem in which to investigate the development of singularities on interfaces driven by a density difference.

2 Formulation of the problem

The vortex sheet that forms at the interface between the fluids may be characterised by its complex position $z(\xi,t) = x(\xi,t) + iy(\xi,t)$, and its strength $V(\xi,t)$, where (x,y) are Cartesian coordinates, t is time and ξ is a Lagrangian parameter determined by the requirement that the velocity at a point on the sheet be the average of the tangential velocities on either side of that point. Thus if the complex velocities on either side of the sheet are denoted by $\bar{q}_+$ and $\bar{q}_-$, and $\bar{q}$ is the complex velocity of the sheet, then (e.g. Moore, 1982)

$$q = \frac{\partial \bar{z}}{\partial t}(\xi,t) = \frac{1}{2}(q_+ + q_-) \ ,$$

where

$$q_\pm = q \pm \frac{1}{2}V(\frac{\partial z}{\partial \xi})^{-1} \ .$$

Moreover, from use of the Biot-Savart law, the velocity of a point on the sheet is given by the Birkhoff-Rott equation:

$$\frac{\partial \bar{z}}{\partial t}(\xi,t) = \frac{1}{2\pi i}\int_0^{\xi_o} \frac{V(\xi',t)\,d\xi'}{z(\xi,t) - z(\xi',t)} \ , \tag{1}$$

where the principal value is taken in the integral, and ξ_o is the Lagrangian length of the interface. Since the interface is periodic, the solutions must satisfy the periodicity conditions

$$z(\xi + \xi_o) = z(\xi), \qquad V(\xi + \xi_o) = V(\xi) \ .$$

The derivation of the equation for $\frac{\partial V}{\partial t}(\xi,t)$ is non-trivial; the details may be found in Baker, Meiron & Orszag (1982) and Moore (1982). The equation is

$$\frac{\partial V}{\partial t}(\xi,t) = (1-\frac{\rho_-}{\rho_+})\left[-\frac{\partial}{\partial \xi}\Re(q_-\frac{\partial z}{\partial t}) + \frac{\partial}{\partial \xi}[\frac{1}{2}\Re(q_-\bar{q}_+) - g\Im(z)]\right] . \qquad (2)$$

When equations (1) and (2) are integrated over the interval $(t, t+dt)$ using a forward stepping Euler's method, for example, it transpires that the new values $z(t+dt)$ and $V(t+dt)$ are given implicitly so that the solution can only be found by iteration. However, when the Boussinesq limit is taken, equation (2) reduces to

$$\frac{\partial V}{\partial t}(\xi,t) = -(1-\frac{\rho_-}{\rho_+})g\,\Im(\frac{\partial z}{\partial \xi}) . \qquad (3)$$

This simplification means that iteration is *not* required since z and V at the new time $(t+dt)$ may readily be found using second or fourth order Runge–Kutta formulae. This is a major motivation for making the Boussinesq approximation.

In order to simplify the equations, the following non-dimensionalisation was adopted:

$$z \to az\ , \qquad V \to 4\pi a\left(\frac{ga\Delta\rho}{\rho_+}\right)^{\frac{1}{2}} V\ , \qquad t \to \left(\frac{a\rho_+}{g\Delta\rho}\right)^{\frac{1}{2}} t\ ,$$

where $\Delta\rho = (\rho_+ - \rho_-)$. Equations (1) and (3) become

$$\frac{\partial \bar{z}}{\partial t}(\xi,t) = -2i\int_0^{\xi_0} \frac{V(\xi',t)\,d\xi'}{z(\xi,t)-z(\xi',t)}\ , \qquad (4)$$

$$\frac{\partial V}{\partial t}(\xi,t) = -\frac{1}{4\pi}\Im(\frac{\partial z}{\partial \xi}(\xi,t)) . \qquad (5)$$

Note that equations (4) and (5) are independent of any Froude number so that the problem is unique.

These coupled integro–differential equations will be solved numerically. A number of initial conditions could be considered. We will study the simple problem where a two–dimensional circular bubble of lighter fluid is instantaneously introduced at $t = 0$. An advantage of this initial condition is that only one half of the bubble needs to be considered because of symmetry about the y-axis. However this restriction could easily be relaxed. Similarly we could study other initial conditions which are easier to model experimentally, e.g. injection of lighter fluid into heavier fluid (cf. Hooper, 1986).

The symmetry conditions for z and V about the y-axis are

$$z(-\xi,t) = -\bar{z}(\xi,t), \qquad V(-\xi,t) = -V(\xi,t),$$

$$z(N+\xi,t) = -\bar{z}(N-\xi,t), \qquad V(N+\xi,t) = -V(N-\xi,t).$$

In order to solve the equations numerically it is necessary to discretise them. The continuous vortex sheet is replaced by $2N$ point vortices with complex position $z_s(t)$ and strength $V_s(t)$ so that there are $(N+1)$ interfacial points in one half of the bubble when both points on the axis of symmetry are included. The parameter s acts as a discrete Lagrangian variable and the points lie on the surface in order of increasing s. Following Moore (1982) we take s to be the discrete set of integers $s = 0, 1, 2, \ldots, 2N-1$. We use central finite differences with respect to s to estimate the derivatives with respect to the continuous Lagrangian parameter ξ. The symmetry conditions about the y-axis

$$z_{-s}(t) = -\bar{z}_s(t), \qquad V_{-s}(t) = -V_s(t),$$

$$z_{N+s}(t) = -\bar{z}_{N-s}(t), \qquad V_{N+s}(t) = -V_{N-s}(t).$$

allow central differencing for the end points.

In order to evaluate the integral in equation (4) numerically, a cancellation function is constructed which models the behaviour of the integrand at its singular point. This cancellation function is then subtracted out numerically and added in analytically. The application of this method to vortex sheets was developed by Van de Vooren (1965). Equations (4) and (5) then become

$$\frac{d\bar{z}_s}{dt} = -2i \sum_{r \neq s} \frac{V_r}{z_s - z_r} + 2i \left[\frac{DV_s}{Dz_s} - \frac{1}{2} \frac{V_s D^2 z_s}{(Dz_s)^2} \right] , \qquad (6)$$

$$\frac{dV_s}{dt} = -\frac{1}{4\pi} \Im(Dz_s) , \qquad (7)$$

where D^p denotes a finite difference estimate of the pth derivative w.r.t. s.

The appropriate initial conditions for a circular bubble instantaneously introduced at $t = 0$ are

$$z(s, 0) = -i \exp(2\pi i s/2N) , \qquad V(s, 0) = 0 .$$

The first term on the RHS of (6) is the velocity induced at the point z_s by a system of isolated point vortices at z_r $(r \neq s)$. It is assumed that the self-induced velocity of a point vortex is zero. The second term is analogous to the Van de Vooren (1965) correction term, and comes from the contribution of the integral around the point z_s. These derivatives were estimated either using interpolation polynomials or by spectral differentiation. The effect of the Van de Vooren term is to improve the accuracy of discretisation from $O(N^{-1})$ to $O(N^{-11})$ when 11–point polynomials are used.

3 The numerical procedure and the calculation of invariants

Only the motion of the right half of the bubble was followed. This required $2(N+1)$ coupled ordinary differential equations to be integrated forward in time.

We used a second order Runge-Kutta method, and after each time step Krasny's (1986) filtering technique was applied to the Fourier series representation of both the sheet position $z(s,t)$ and the point vortex strength $V(s,t)$. The Fourier series were computed using a FFT based on the Cooley-Tukey method. To check on the accuracy of the computations, the potential energy, Ω, kinetic energy, T and total energy, $(\Omega + T)$ were calculated together with the area, A, of the bubble. Both total energy and area should remain constant. After non-dimensionalisation the quantities Ω, T and A are equal to

$$\Omega = \int_0^N y_s^2 \frac{dx}{d\xi} \, d\xi \ , \tag{8}$$

$$T = -4\pi \int_0^N \left[\int_0^\xi V d\xi \right] \Im(q \frac{dz}{d\xi}) \, d\xi \ , \tag{9}$$

$$A = 2 \int_0^N y \frac{dx}{d\xi} \, d\xi \ , \tag{10}$$

where y_s denotes the bubble surface, and use has been made of the symmetry of the problem. The integrals were evaluated using the trapezoidal rule which is exponentially accurate for periodic integrals (e.g. Conte and de Boor, 1965). The sheet strength, γ, is given by

$$\gamma = V |\frac{dz}{d\xi}|^{-1} \ ,$$

and the curvature, C, by

$$C = \frac{\Im \left(\frac{d\bar{z}}{d\xi} \frac{d^2 z}{d\xi^2} \right)}{|\frac{dz}{d\xi}|^3} \ .$$

The computations were performed with N = 32, 64, 128, 256 and dt = 0.01, 0.005, 0.001, 0.0005, 0.0001 in single precision (13 digits) on a Cray-1 using a second order Runge–Kutta method and a filter level of 10^{-13} at each time step. Figure 1 illustrates the sheet position, sheet strength and curvature for $N = 128$ and $dt = 0.001$. As the bubble rises, the lower surface moves more rapidly than the upper surface, and the upper half of the bubble begins to expand. At $t \approx 1.69$ the sheet strength forms what appears to be a cusp point, while the curvature seems to develop an infinite jump discontinuity. The singularities form at points on the interface where the vortex sheet is continually being compressed. In other regions of the bubble, particularly the upper surface, the sheet is being stretched and remains smooth and stable. This agrees with the observation that vortex sheets do not appear to exhibit Helmholtz instability in areas of rapid stretching (Moore and Griffith-Jones, 1974).

At $t = 1.65$, i.e. shortly before the critical time $t_c \approx 1.69$ (see below), the absolute error in energy conservation was 2.506×10^{-7} and the relative error in area 1.153×10^{-11}; thus a high degree of accuracy was maintained suggesting that the numerical solution was reliable. At times even closer to the critical time, these values deteriorated rapidly. Beyond the critical time (which depended on N and dt), the solution was no longer smooth and was considered meaningless. The functions $z(\xi, t)$ and $V(\xi, t)$ are then no longer analytic. Consequently the Birkhoff-Rott equation (1) is no longer valid and the Van de Vooren term in (6) has become infinite at a point on the sheet. As $t \to t_c$, we found that both the arclength and the sheet strength at the cusp point remained finite, as in the related problems studied by Meiron *et al.* (1982), Krasny (1986), Rottman *et al.* (1987), Shelley (1992) and Rottman & Stansby (1992) (cf. Higdon & Pozrikidis (1985) who suggested that the sheet strength became infinite at the critical time).

If the maximum curvature, C_{max}, becomes infinite as $t \to t_c$ then an estimate of t_c can be found by plotting C_{max}^{-1} versus time (Higdon and Pozrikidis, 1985). Figure 2 shows clearly that C_{max}^{-1} tends to zero as $t \to t_c$. The critical time t_c can be estimated quite accurately by drawing a straight line through the points for which the solution was known to be accurate and reliable. For $N = 128$ and $dt = 10^{-3}$ this gave $t_c \approx 1.695$. The convergence of the numerical solution as $dt \to 0$ for fixed N, and $N \to \infty$ for fixed dt, is shown in figure 3.

Table 1 shows the values of t_c calculated in this way for various N and dt. The most accurate results seem to be obtained with $dt = 10^{-3}$. For this choice of step size, t_c^N was fitted to the expression (Krasny, 1986):

$$t_c^N = t_c^\infty + \frac{\alpha}{N} ,$$

where t_c^∞ is the extrapolated critical time as $N \to \infty$. A plot of t_c^N against N^{-1} gave a straight line, and from this t_c^∞ and α were estimated using a linear least squares fit; we found

$$t_c^\infty = 1.689 \qquad \text{and} \qquad \alpha = 0.771 .$$

Table 2 gives the times τ_z, τ_V at which the filtering technique was switched off for $z(\xi, t)$ and $V(\xi, t)$ respectively. Following Rottman *et al.* (1987) we fit values of τ_z^N, τ_V^N to the expressions

$$\tau_z^N = \tau_z^\infty - \frac{\alpha_z}{N}, \qquad \tau_V^N = \tau_V^\infty - \frac{\alpha_V}{N}.$$

The values τ_z^∞, α_z and τ_V^∞, α_V were estimated using a least squares fit. For $dt = 0.001$ we obtained

$$\tau_z^N = 1.70 - \frac{7.36}{N}, \qquad \tau_V^N = 1.70 - \frac{2.50}{N}.$$

Thus to three significant figures $\tau_z^\infty = \tau_V^\infty = 1.70$, which is close to the critical time $t_c^\infty = 1.689$. In fact, $\tau_z^\infty, \tau_V^\infty$ must be greater than t_c^∞ for the following reason. If the Fourier coefficients of position decay at the critical time like $k^{-\mu}$ as $k \to \infty$, then they must decrease to zero as $k \to \infty$. The value τ_z^∞ corresponds to the time at which every coefficient has reached the filter level (here 10^{-13}), which must be after the critical time t_c^∞. A similar argument holds for τ_V^∞.

The computations were repeated with $N = 128$, a time step $dt = 10^{-4}$, and filtering every time step (filter level 10^{-13}). A slightly surprising result emerged in that both the critical time and the time at which the filtering was switched off were increased by approximately 0.015 time units. However, filtering every ten time steps with $dt = 10^{-4}$, gave virtually identical results to those obtained filtering each time step with $dt = 10^{-3}$. Thus if dt is chosen sufficiently small for the second order Runge–Kutta method to be accurate, the solution depends on two numerical parameters, namely N and $F\,dt$ where F is the number of time steps after which filtering is applied.

Filtering may be regarded as a smoothing process which removes energy from the system. Using $dt = 10^{-4}$ and $F = 1$ involves filtering ten times more often than if $dt = 10^{-3}$ and $F = 1$. The increase in t_c^∞, etc., created by repeatedly filtering seems to be generated during the initial stages of the bubble's motion, i.e. while the velocities are small. The Fourier modes filtered are those of complex position. A mode which is *slightly greater* than the filter level after one time step of 10^{-3} will be approximately one tenth the size after a time step of 10^{-4}, i.e. *less* than the filter level and hence removed. Indeed, in the extreme instance of very small time steps and filtering applied every time step, the interface would not move at all because none of the modes would ever have sufficient time to grow above the filter level. We conclude that the solution is dependent on N and the time interval after which the filtering is applied. Convergence as $dt \to 0$ can be obtained as long as $F\,dt$ is kept constant. In our calculations the filtering cut-off times and critical time began to diverge for $F\,dt < 0.001$; thus only solutions with $F\,dt \geq 0.001$ are discussed below.

4 The asymptotic behaviour of the Fourier series

The properties of a periodic function's singularities can be identified by examining the asymptotic properties of the function's Fourier series, e.g. Sulem, Sulem and Frisch (1983) (hereafter referred to as SSF) and Krasny (1986). In particular, suppose we extend z into the complex ξ–plane by analytic continuation. Then the nature of the singularities closest to the real ξ–axis determine the high wavenumber asymptotic behaviour of the Fourier coefficients (e.g. Carrier, Krook and Pearson, 1966). Suppose that for $|\xi - \xi_s(t)| \ll 1$, the function $z(\xi, t)$ has the local behaviour

$$z(\xi,t) = A_0 + A_1(\xi - \xi_s) + A_2(\xi - \xi_s)^2 + \ldots + \alpha(t)\ (\xi - \xi_s)^{\mu(t)} + \ldots\ , \quad (11)$$

where

$$\xi_s(t)) = \xi_r(t) + i\delta(t)\ ,$$

$\mu(t)$ and α are complex, $\Re(\mu(t)) > -1$, $\delta(t) > 0$, and $\delta(t)$ is the branch point nearest to the real ξ–axis in the upper half plane. In this example a derivative of z is infinite at $\xi = \xi_s$ if μ is not an integer. A physical singularity occurs in a numerical calculation on the real ξ–axis when the arc traced out by $\xi_r(t) + i\delta(t)$ first crosses the real ξ–axis, i.e. when $\delta(t) = 0$. Carrier, Krook and Pearson (1966) show that the Fourier coefficients $a(k,t)$ behave asymptotically like

$$a(k,t) \sim C(t)e^{-k\delta(t)}k^{(-\mu(t)-1)}\exp(2\pi i\xi_r(t)k/2N) \ , \tag{12}$$

as $k \rightarrow \infty$, where k is wavenumber. Thus when the solution is analytic on the real ξ–axis, i.e. when $\delta > 0$, the coefficients decay exponentially, but when the solution has a singularity on the real ξ–axis then the coefficients decay algebraically like $k^{-\Re(\mu(t)+1)}$. By examining the Fourier coefficients for large k carefully, it is in principle possible to estimate $\delta(t)$, $\mu(t)$, etc.. However, a potential difficulty is that $\mu(t)$ can change discontinuously if two singularities collide. For example, SSF showed that in the case of shock formation in the kinematic wave equation, the algebraic component of decay for $t < t_c$ is $k^{-\frac{3}{2}}$, but for $t = t_c$ it is $k^{-\frac{4}{3}}$.

If there is only one singularity closest to the real ξ–axis, then we have that as $k \longrightarrow \infty$

$$\log|a(k,t)| \approx R - k\delta - (\Re(\mu) + 1)\ \log\ k \ ,$$

where $R = \log|C|$. SSF and Krasny (1986) used a linear least squares fit to estimate R, δ and $\Re(\mu)$ from their numerical results. They found that for $|t - t_c| \ll 1$, the decay of the Fourier spectrum for large $k \gg \delta^{-1}$ is predominantly exponential, but for $1 \ll k \ll \delta^{-1}$ the decay is algebraic. Thus fitting to very high wavenumbers at times when $|t - t_c| \ll 1$ gave values for $\delta(t)$, while fitting for moderately large wavenumbers yielded $\Re(\mu(t))$. Of course t_c is fixed by $\delta(t_c) = 0$.

A slight complication in the present analysis is that due to the symmetry of the bubble problem, singularities arise at $(\xi_r + i\delta_1)$ and at $(-\xi_r + i\delta_1)$. In addition there are two further singularities at $(\xi_r - i\delta_2)$ and $(-\xi_r - i\delta_2)$ where we have assumed that $\delta_j > 0$ but not that $\delta_1 = \delta_2$. The asymptotic behaviour of the Fourier coefficients for $k \gg 1$ depends only on the singularities in the upper half plane (UHP), while the behaviour for $k \ll -1$ depends only on those in the LHP. The asymptotic form for two symmetric singularities was shown by Pugh (1989) to be

$$\log|a(k,t)| \approx R - k\delta - (\Re(\mu) + 1)\log(k) + M \ , \tag{13}$$

where

$$M = \log|\cos(\beta k + \Im(\mu)\log(k) + \phi)|$$

and $\beta = 2\pi\xi_r/N$.

For convenience we define the 'enclosing envelope' of a Fourier spectrum to be the function given by the right hand side of (13) without the term M. This function decreases monotonically with increasing k. When $\log_{10}|a(k,t)|$ was plotted against k it was found that the Fourier coefficients for z oscillated (see figure 4a). This modulation arises because of the term M in equation (13). The enclosing envelope of the spectrum yields a straight line before the critical time. The decay is therefore exponential and the solution analytic. When $\log_{10}|a(k,t)|$ was plotted against $\log_{10} k$ (figure 4b), a straight line representing the 'enclosing envelope' could be drawn at $t \approx 1.695$ for $N = 128$; this corresponds to algebraic decay and hence a singularity. In order to obtain values for R, δ, β, μ and ϕ for times close to the critical time, we tried a least squares fit of the numerical results to equation (13). However this failed to converge even with apparently good initial guesses.

A second method, referred to here as a 'global method', was reasonably successful in estimating the enclosing envelope of the Fourier spectrum. To do this μ was taken to be real. Quadratic interpolation was used to estimate the maxima of each 'hump' and a linear least squares fit used on these maxima to obtain R, δ and μ. Expression M was then calculated and inverted to give a straight line of slope β and intercept ϕ. The estimates for δ, β and ϕ were seemingly reliable, i.e. they did not vary significantly with the range of wavenumbers used, whereas this was not true for μ. Since one of the main aims of our calculations was to determine the form of the singularity, an accurate method of obtaining μ was required. Eventually we settled on the 'local method' described in the next section.

5 Local method for fitting to Fourier series coefficients

In this approach we fitted equation (13) exactly to six consecutive values of $|a(k)|$, e.g. $|a(l)|$ for $k-2 \le l \le k+3$.[1] This was done for a number of values of k in a range $k_{min} < k < k_{max}$, and then we sought consistency in $R(k)$, $\delta(k)$, etc. over the range of values of k. The six unknowns were determined using a NAG routine which found roots of non-linear equations using a Newton iteration. Since the NAG routine did not usually converge unless the starting values were 'close' to the solution, initial estimates of the solution were obtained from the 'global' method. The solutions for the unknowns generated for k were used as starting values for $k+1$.

This method was applied to a run with $N = 128$ and $dt = 0.001$ at times $t = 1.65\,(0.01)\,1.70$ (the estimated singularity time is 1.69). A filter level of 10^{-13} was used with 14-digit arithmetic. Initially we assumed that μ was real in line with Moore's (1979) result. However, while the values for β and ϕ were fairly consistent to three decimal places, those for R, δ and μ were much more

[1] Six values of $a(k)$ were required since the Fourier coefficients are purely imaginary due to the symmetry of the problem.

erratic (e.g. see figure 5a). On the other hand, when the same data was fitted allowing μ to be complex, the plot of $\Re(\mu)$ versus k illustrated in figure 5b was significantly less erratic. This was despite the fact the $\Im(\mu)$ was relatively small; in fact $|\Im(\mu)| \leq 0.03$ which turns out to be approximately the same size as the error in our final estimate of $\Re(\mu)$. Although as $t \to t_c$, i.e. $\delta \to 0$, the values of $\Re(\mu(t))$ did not change significantly with time, no consistency in $\Re(\mu)$ was obtained with k.

Next, the computations were repeated with 28-digit arithmetic and a filter level of 10^{-28}. Plots of sheet position, sheet strength versus arclength, and curvature versus arclength were graphically indistinguishable from those obtained using 14-digit arithmetic (see figure 1). For $N = 128$ and $dt = 0.001$, the algebraic decay $\Re(\mu)$ plotted against k at a time $t = 1.65$ is illustrated in figure 6a. The values for $\Re(\mu)$ for $5 < k < N/2$ decrease slowly and appear to tend towards 1.5 as $k \to \infty$. This value of $\Re(\mu)$ corresponds to the same type of singularity as described by Moore (1979). The reason why there is little consistency in the values of $\Re(\mu)$ for $k > N/2$ is discussed below.

Since $z(\xi)$ is complex, $a(-k)$ neither equals $a(k)$ nor it's complex conjugate. Hence fresh information can be found by fitting (13) to $a(-k)$. The results for $k < 0$ are more consistent than those for $k > 0$. Figure 6b shows that $\Re(\mu)$ is again very close to 1.5 for $5 < |k| < N/2$, although there is again no consistency for $|k| > N/2$. In figure 7 we have plotted the exponential decay, $\delta(k)$, of the Fourier coefficients as a function of both positive and negative wavenumbers k. Again, the coefficients for $k < 0$ yield a more consistent value of δ at each time level than those for $k > 0$.

In order to assess the relative importance of precision and filter level, the computations were repeated with 28-digit arithmetic but a filter level of 10^{-13}. The results obtained for $\Re(\mu)$ versus k were identical to those using 14-digit arithmetic and a filter level of 10^{-13}. These results were not significantly affected when the filter level was increased from 10^{-28} to 10^{-18}. However, as the filter level was increased further from 10^{-18} to 10^{-13}, the consistency in $\Re(\mu)$ deteriorated (see figure 8). These results emphasise that the correct combination of filter level and arithmetic precision must be used in order to obtain accurate results.

The effect of doubling the number of points was also examined. For a run with $N = 256$, $dt = 0.001$, 28-digit arithmetic and a filter level of 10^{-28} we found that at $t = 1.65$, the results were consistent up to $k = k_a \approx 120$, i.e. approximately twice as many modes were accurate as in the $N = 128$ calculation. The ratio of k_a/N appears to be about $\frac{1}{2}$ for this problem. Figure 9 illustrates $\Re(\mu)$ versus k for both $k > 0$ and $k < 0$ at the extrapolated critical time of 1.689 for different N.

In figure 10 we have plotted the values of $\Re(\mu)$ obtained for $k < 0$ at several times close to the critical time. The consistency for $|k| \leq N/2$ is evident except at $t = 1.70$, i.e. after the critical time. However, the 'average' value of $\Re(\mu)$ slowly increases as $t \to t_c$, so that at $t = 1.69$ the average value is slightly greater than 1.6. It is not clear whether this change in $\Re(\mu)$ is genuine or merely due to the breakdown of the calculations as $t \to t_c$ (see below). A decrease in the slow drift might be achieved by including higher–order corrections in (11) and (13) (see Shelley (1992) for further details).

We emphasise that one of our main aims is to obtain an accurate estimate of $\Re(\mu)$ at $t = t_c$, since this will tell us what the form of the physical singularity is on the ξ–axis. However, as indicated above a potential difficulty is the fact that for a number of problems it is known that the value of $\Re(\mu)$ can change from one value at $t < t_c$ to another at $t = t_c$. This occurs if singularities collide. An example is the kinematic wave equation with suitable initial conditions. For example the problem

$$\frac{\partial u}{\partial t} + u\frac{\partial u}{\partial x} = 0 \ , \qquad u(x,0) = -\sin x \ ,$$

is well known to develop a shock at $t = t_* = 1$. SSF have shown that the Fourier spectrum $\hat{u}_k$ has the asymptotic behaviour

$$\hat{u}_k \approx k^{-\frac{3}{2}} e^{\delta(t)k} \qquad \text{for} \qquad t < t_* \ ,$$

but

$$\hat{u}_k \approx k^{-\frac{4}{3}} \qquad \text{for} \qquad t = t_* \ .$$

Note the change in the value of μ from $\frac{1}{2}$ to $\frac{1}{3}$.

The slow increase in $\Re(\mu)$ as $t \to t_c$ possibly suggests that a similar snap change occurs here. Fortunately, a slight modification of the analysis of Cowley, Baker, Tanveer & Page (1992) for a vortex sheet allows us to show that the singularity in question does not change form at $t = t_c$. Following these authors assume that at $t = t_c$ the singularity develops at $\xi = \xi_c$, and write $z_c = z(\xi_c, t_c)$ and $V_c = V(\xi_c, t_c)$. For $0 < t_c - t \ll 1$ and $|\xi - \xi_c| \ll 1$, we propose the following asymptotic expansions:

$$z = z_c + (t_c - t)(a_1 + a_2\zeta) + (t_c - t)^{\bar{\mu}} f(\zeta) + \dots \ , \tag{14}$$

$$V = V_c + (t_c - t)(a_3 + a_4\zeta) + (t_c - t)^{\bar{\mu}} g(\zeta) + \dots \ , \tag{15}$$

where

$$\zeta = \frac{\xi - \xi_c}{t_c - t} \tag{16}$$

is a local similarity variable, f and g are functions of the similarity variable, and $\bar{\mu}$ and the a_j are constants. In what follows we assume for convenience that $1 < \bar{\mu} < 2$; in due course we will identify $\bar{\mu}$ with μ in (11). On substituting into (5) we find that

$$\Im(a_2) = 4\pi a_3 \ , \qquad \Im(f') = -4\pi(\zeta g' - \bar{\mu}\zeta) \ .$$

Similarly from careful consideration of (4) it follows that

$$a_1 = 2i\int_0^{\xi_o} \frac{V(\xi',t_c)}{z(\xi,t_c)-z(\xi',t_c)}d\xi' \ ,$$

and

$$s\bar{f}' - \bar{\mu}\bar{f} = \frac{2iV_c}{a_2^2}\int_{-\infty}^{\infty}\frac{f'(u)}{\zeta - u}du \ . \tag{17}$$

The solution to this equation (Cowley *et al.*, 1992) is

$$f = (1-i)a_r e^{i\theta}\left(1+\frac{|a_2|^4\zeta^2}{4\pi^2V_c^2}\right)^{\frac{\bar{\mu}}{2}}\sin\left(\bar{\mu}\arctan\frac{|a_2|^2\zeta}{2\pi V_c}\right) \ , \tag{18}$$

where a_r is a real constant and

$$2\theta = -\arg\left(\frac{V_c}{a_2^2}\right) \ .$$

An important property of (18) is that for $0 < t_c - t \ll 1$, there are branch–point singularities of power $\bar{\mu}$ located in the complex ξ plane at $\zeta = \pm 2\pi i|a_2|^{-2}V_c$, i.e. at

$$\xi = \xi_c \pm 2\pi i|a_2|^{-2}V_c(t_c - t) \ .$$

At $t = t_c$, the inner region described by the similarity variable collapses to zero width, and a singularity of power $\bar{\mu}$ forms on the real ξ–axis. From matching with an outer solution we conclude that as $\xi \to \xi_c$ this has the form

$$z = z_c + a_2(\xi-\xi_c) + (1-i)a_r e^{i\theta}\mathrm{sgn}(V_c(\xi-\xi_c))\left|\frac{a_2^2(\xi-\xi_c)}{2\pi V_c}\right|^{\bar{\mu}}\sin(\frac{\pi\bar{\mu}}{4}) + \dots \ .$$

Therefore, if we can estimate $\bar{\mu}$ from the solution in the complex ξ–plane for $t < t_c$, we can be confident that the singularity does not change its character on hitting the real ξ–axis.

However, there is still the need to address why there is the fall off in the estimate of the coefficients for $|k| \geq N/2$. This fall–off is robust in the sense that it occurs no matter what numerical method is used to solve the discretised equations. For instance:

1. No improvement in the estimate of $\Re(\mu)$ was obtained when the computations were repeated using a fourth order Runge-Kutta method. Of course for a fixed dt, the energy and area conservation were improved significantly and the values for z, V and the Fourier coefficients differed by an amount $O(dt^3)$. However, using second order rather than fourth order Runge-Kutta had no effect on the values of $\Re(\mu)$, although the values of the constant in (13) changed slightly.

2. The initial distribution of point vortices around the circle was varied. For instance, rather than using a uniform distribution, the point density in the neighbourhood of ξ_c was increased. We hoped that the resolution and accuracy would be improved; instead we found that the estimates of $\Re(\mu)$, etc. were, if anything, worse.

3. More sophisticated filtering methods were tried. For instance, rather than setting a Fourier mode to zero when it is less than the filter level, we tried fitting a 'tail' to the Fourier coefficients using information from the Fourier coefficients with magnitudes greater than the filter level (see also Cowley, Duck & Tutty (1992)). Again, no improvement was obtained.

4. As $t \to t_c$ the Van de Vooren term becomes very large at the singular point on the sheet. The error in the velocity using any time stepping scheme therefore becomes arbitrarily large in the region of the singularity. A number of checks were applied to assess this effect.

   (*a*) We evaluated the derivatives in the Van de Vooren term using Fourier series rather than using high-order interpolation polynomials. This has an advantage that for analytic functions the error falls off faster than any algebraic power of N. However, as the critical time is approached, spectral differentiation loses accuracy as significant errors appear from aliasing. Indeed, at $t = t_c$ the Fourier series of the Van de Vooren correction term is divergent.

   (*b*) We performed a number of runs in which we simply omitted the Van de Vooren term. The growth rate of the instabilities is then decreased (Moore, 1981), with the result that the singularity time is delayed. Of course the accuracy as monitored by the total energy and area was significantly worse, i.e. $\Delta E = O(10^{-2})$ as opposed to $O(10^{-8})$ at $t = 1.5$, but again no significant change was observed in the predicted values of $\Re\mu$.

   (*c*) Rather than just omitting the Van de Vooren term, we modified our scheme to the (spatially) spectrally accurate method developed by Sidi and Israeli (1988) and used by Shelley (1992). An advantage of this method is that for the uniform vortex sheet, the growth rates of linear modes are predicted exactly. This contrasts with the standard point vortex method, with or without the Van de Vooren term, which artificially reduces the growth rates of the most unstable modes. An additional advantage of the scheme is that computational times are halved. However a significant improvement in the estimate of $\Re(\mu)$ was not observed. This is possibly not surprising since in our earlier calculations sufficiently high order polynomials were used so that the truncation error was smaller than the rounding error. In addition, while the alternate point rule is (formally) spatially spectrally accurate for $t < t_c$, that is not true at the moment the singularity forms.

We also note that the system of equations for $\Re(\mu)$ is ill-conditioned as $|k| \to \infty$ (Pugh 1989). However while this may be one reason why there is a deterioration in the estimates of $\Re(\mu)$ for $|k| > N/2$, we believe that the major reason is that the asymptotic behaviour of the Fourier coefficients given by equation (13) is valid for the coefficients, a_k^∞, of the *infinite* Fourier series. In the discretised problem using N modes, the discrete Fourier coefficients a_k^N are only an accurate representation of a_k^∞ for $|k| << N$. The reason for this can be readily understood by recalling that the a_k^N are given by a (spectrally accurate) trapezoidal approximation to an integral. For large $|k|$, the integrand oscillates rapidly with the result that a_k^N is not a good approximation to a_k^∞ even though the Fourier *sum* is spectrally accurate for analytic functions. It is therefore inappropriate to fit (13) to a_k^N for $|k| = O(N)$; in practice the fit seems to work for $|k| < N/2$. This conclusion is consistent with the observation that twice as many modes gave accurate values for $\Re(\mu)$ when N was doubled. This error, coupled with the ill-conditioning in the system of equations for $\Re(\mu)$, gives rise to the rapid deterioration in the estimates for $|k| > N/2$. A method for overcoming this problem, at least for the kinematic wave equation and other equations with quadratic nonlinearity, is described by Tutty & Cowley (1992).

6 Discussion and conclusions

The equations of evolution for the rise of a two-dimensional Boussinesq bubble have been integrated forward in time until a singularity occurs. Evidence has been presented which suggests that at two symmetric points on the interface the curvature becomes infinite, and the sheet-strength develops a cusp-point. An accurate estimate of the non-dimensional critical time, $t_c^\infty \approx 1.689$, has been found.

Using the asymptotic form of the Fourier coefficients (13) we can explain the modulated behaviour of the Fourier series. In addition we can determine the time at which the singularity occurs and the algebraic decay of the Fourier coefficients with wavenumber. In order to obtain accurate results, especially for μ, both sufficient precision and a suitable filter level need to be used (Krasny, 1986; Pugh, 1989). In particular, for a run with $N = 128$ and $dt = 0.001$ consistent values for $\Re(\mu)$ were only obtained when the filter level was smaller than 10^{-18} and μ was taken to be complex. As the filter level was increased from 10^{-18} to 10^{-13} the consistency in the estimate of μ was gradually lost.

We find that the Fourier coefficients $a(k)$ for $k < 0$ gave considerably better results than those for $k > 0$. As yet no explanation can be given as to why this is the case, although a possibility is that there is better cancellation in the higher order terms in the asymptotic Fourier series for z in the case $k < 0$ than for $k > 0$. If so, including higher order terms in (11) and (13) should lead to an improvement of the results, especially for $k > 0$ (see Shelley, 1992). Pugh (1989) has found examples of problems where results are more consistent for

$k > 0$ than $k < 0$.

The loss of consistency for $\Re(\mu)$ versus k for $|k| > N/2$ is due to fitting an asymptotic formula valid for an *infinite* Fourier series to a *finite* Fourier series. We find that for $k < 0$ and $5 < |k| < N/2$, $\Re(\mu) = 1.53 \pm 0.03$. This decay rate is the same as that obtained analytically by Moore (1979) for small sinusoidal disturbances to a parallel shear flow, and suggests that the singularity has the same form.

The method of fitting exactly to sequences of six consecutive Fourier coefficients appears to be an improvement on previous authors' methods of using a least squares fit over a range of wavenumbers. The value of $\Re(\mu) = 1.53 \pm 0.03$ is closer to the theoretical value of 1.5 than those obtained by many other authors; Shelley (1992) has obtained similar accuracy.

The rise of the two–dimensional Boussinesq bubble has been studied before. For instance the formulation and non-dimensionalisation used by Rambaldi and Randall (RR) is almost identical to that here; the only difference is a multiplicative factor of 4π in the sheet strength. RR used a second order Runge-Kutta method, but repositioned their point vortices rather than filtered. They confirmed convergence of their solution with increasing N at the initial time $t = 0$, but not at later times. Hence, while a comparison with their results for $t \leq 1.7$ shows qualitative agreement, we believe that their results for $t > t_c$ are spurious. In particular, although their calculations *appear* acceptable for $t \geq t_c$, we believe that this is because of their use of repositioning. Indeed, as Moore (1981) has observed, 'smoothing or repositioning can yield an acceptable solution when none, in fact, exists'. An advantage of filtering is that the breakdown of the numerical solution is very evident, since the vortex nearest to the point at which the singularity forms 'flies off' the sheet for $t > t_c$. When repositioning is used, the points are 'constrained' to remain equidistant, and the breakdown is less obvious. Moreover, on the basis of the conclusions of Krasny (1986) and Rottman *et al.* (1987), it is anticipated that no convergence would be found in the results of RR after the critical time.

In addition Anderson (1985) has used a vortex blob method to solve this problem. As the desingularisation parameter, $\hat{\delta}$, tends to zero, the discretised equations for the vortex blob method with fixed N converge to (6) but without the Van de Vooren term. Anderson (1985) conjectured that as $\hat{\delta} \to 0$, the arclength becomes infinite as a singularity was approached. According to the results presented here, this does not appear to be the case. It can be shown that the time units of Anderson, t^A, and those here, t^P, are related by

$$t^P = \sqrt{2}\, t^A.$$

The critical time predicted here is $t_c^P = 1.689$ which corresponds to $t_c^A = 1.194$. Anderson (1985) estimated the critical time to be $t_c^A = 1.0$ on the basis that at this time the arclength behaved like $\hat{\delta}^{-0.105}$. The critical time predicted here is larger then this. Moreover it is possible to clearly demonstrate convergence and a finite arclength at $t_c^A = 1.0$ (see Pugh (1989) for further details).

Although we have concentrated on a specific problem, we believe that our results are robust. In particular we believe that singularities will develop for a wide range of initial conditions, and that our results are not an artifact of, for instance, the symmetric initial conditions. (However we note that singularity formation could possibly be suppressed if the vortex sheet was excessively stretched, e.g. as a result of rapid injection of one fluid into the other.) This view is supported by the existence of the local similarity form (18) of the singularity. Moreover, in the case of perturbations to a vortex sheet, Cowley *et al.* (1992) show that branch-cut singularities of power $\frac{3}{2}$ have a tendency to form in the complex ξ–plane at $t = 0$, and that these singularities can then propagate onto the real ξ–axis. A similar analysis should be possible here confirming that $\bar{\mu} = \frac{3}{2}$ will be the preferred power of singularity as a result of being fixed by the initial conditions. We also note that Pugh (1989) numerically identifies the same singularity power in a number of other density–driven flows, e.g. Rayleigh–Taylor instability, the descent of a vortex pair towards a stable interface, and the rise of an axisymmetric bubble. Indeed, Jennings (1992, private communication) has confirmed that a local singularity structure similar to that of (18) can be found for the axisymmetric vortex sheet formulation.

Finally we note that the formation of singularities is an artifact of the model. There are a number of physical properties of the fluid that have been neglected, e.g. viscosity and surface tension. When these are included the singularities will at least be modified, and may well be eliminated. (That surface tension may not completely eliminate the singularities is supported by Yang (1992) who claims to find singularities in the interface shape for the rise of a vacuous bubble in a two–dimensional channel.) Certainly the development of singularities implies that simple inviscid models involving vortex sheets have limited validity in time, and calculations involving them should be carefully tested for convergence. As Krasny (1986) suggests, in physical terms the development of singularities probably indicates the onset of the roll–up of the vortex sheet.

The authors are very grateful to Prof D.W. Moore both for suggesting the problem in the first place, and for many stimulating discussions. The University of London Computing Centre are thanked for moderate amounts of time on a Cray-1, and very large amounts of time on their Amdahl mainframe. This work was presented at the 30th British Theoretical Mechanics Colloquium, 11-15 April 1988, Imperial College, London. DAP is grateful to the Science and Engineering Research Council for support during the writing of his thesis (Pugh, 1989), of which this is part. DAP also gratefully acknowledges support from the Army Research Office, grant number DAAL03-91-G-0162 while writing this paper.

References

[1] Anderson, C.R. 1985 A vortex method for flows with slight density variations. *J. Comp. Phys.* **61**, 417

[2] Baker, G.R., Meiron, D.I. and Orszag, S.A. 1982 Generalised vortex methods for free surface flow problems. *J. Fluid Mech.* **123**, 477

[3] Baker, G.R. and Moore, D.W. 1989 The rise and distortion of a two-dimensional gas bubble in an inviscid liquid. *Phys. Fluids* **A1** (9), 1451

[4] Baumel, R.T., Burley, S.K., Freeman, D.F., Gammel, J.L. and Nuttall, J. 1982 The rise of a cylindrical bubble in an inviscid liquid. *Can. J. Phys* **60**, 999

[5] Caflisch, R.E. & Orellana, O.F. 1986 Long time existence for a slightly perturbed vortex sheet. *Comm. Pure Appl. Math.* **39**, 807-838.

[6] Caflisch, R.E. & Orellana, O.F. 1989 Singular solutions and ill-posedness for the evolution of vortex sheets. *SIAM J. Math. Anal.* **20**, 293-307.

[7] Carrier, G.F., Krook, M. and Pearson, C.E. 1966 Functions of a complex variable. McGraw Hill 255

[8] Chorin, A.J. and Bernard, P.S. 1973 Discretisation of a vortex sheet with an example of roll-up. *J. Comp. Phys.* **13**, 423

[9] Conte and de Boor 1965 *Elementary Numerical Analysis.* McGraw Hill

[10] Cowley, S.J., Baker, G.R., Tanveer, S. and Page, M.A. 1992 An asymptotic description of the formation of a Moore singularity in a vortex sheet. *In Preparation.*

[11] Cowley, S.J., Duck, P.W. and Tutty, O.R. 1992 The development of finite-time singularities in the unsteady triple-deck equations: Numerical solutions. *In Preparation.*

[12] Higdon, J.J.L. and Pozrikidis, C. 1985 The self-induced motion of vortex sheets. *J. Fluid Mech.* **150**, 203

[13] Hill, F.M. 1975 A numerical study of the descent of a vortex pair in a stably stratified atmosphere. *J. Fluid Mech.* **71**(1), 1

[14] Hooper, A.P. 1986 A study of bubble formation at a submerged orifice using the boundary element method. *Chem. Eng. Sci.* **41**, 1879-1890.

[15] Krasny, R. 1986 A study of singularity formation in a vortex sheet by the point vortex method. *J. Fluid Mech.* **167**, 65

[16] Meiron, D.I., Baker, G.R. and Orszag, S.A. 1982 Analytic structure of vortex sheet dynamics. Part 1. Kelvin-Helmholtz instability. *J. Fluid Mech.* **114** 283

[17] Meng, J.C.S. and Thompson, J.A.L. 1978 Numerical studies of some non-linear hydrodynamics problems by discrete vortex elements methods. *J. Fluid Mech.* **84**, 433

[18] Moore, D.W. and Griffith-Jones, R. 1974 The stability of an expanding circular vortex sheet. *Mathematika* **21**, 128

[19] Moore, D.W. 1979 The spontaneous appearance of a singularity in the shape of an evolving vortex sheet. *Proc. R. Soc. Lond.* **A365**, 105

[20] Moore, D.W. 1981 On the point vortex method. *SIAM J. Sci. Stat. Comput.* **2**(1), 65

[21] Moore, D.W. 1982 A point vortex method applied to interfacial waves. In "Vortex Motion" (H.G. Hornung and E.A. Muller, Eds) Braunschweig/Weisbaden: Viewag and Sohn

[22] Pugh, D.A. 1989 Development of vortex sheets in Boussinesq flows - formation of singularities. *Ph.D. thesis* Imperial College of Science and Technology, London.

[23] Rambaldi, S. and Randall, D.A. 1981 Quasi-Lagrangian models of nascent thermals. *Monthly Weather Review* **109**, 1939

[24] Rottman, J.W., Simpson, J.E. and Stansby, P.K. 1987 The motion of a cylinder of fluid released from rest in a cross flow. *J. Fluid Mech.* **177**, 307.

[25] Rottman, J.W. and Stansby, P.K. 1992 On the 'δ equations' for vortex sheet evolution. *To appear in J. Fluid Mech.*.

[26] Scorer, R.S. 1958 *'Natural Aerodynamics'* Oxford: Pergamon Press.

[27] Siegel, M. 1989 An analytical and numerical study of singularity formation in the Rayleigh-Taylor problem. Ph.D. Thesis, New York University.

[28] Shelley, M. 1992 A study of singularity formation in vortex sheet motion by a spectrally accurate vortex method. *Submitted to J. Fluid Mech.*.

[29] Sidi, A. and Israeli, M. 1988 Quadrature methods for periodic singular and weakly singular Fredholm integral equations. *J. Sci. Comp.* **3**, 201

[30] Sulem, P., Sulem, C., Bardos, C., Frisch, U. 1981 Finite time analyticity for the two and three dimensional Kelvin-Helmholtz instability. *Comm. Math. Phys.* **80**, 485–516.

[31] Sulem, P.L., Sulem, C. and Frisch, H. 1983 Tracing complex singularitics with spectral methods. *J. Comp. Phys.* **50**, 138

[32] Tutty, O.R. and Cowley, S.J. 1992 On using the asymptotic behaviour of finite Fourier series to identify singularities. *In Preparation.*

[33] Van de Vooren, A.I. 1965 (pub. 1980) A numerical investigation of the rolling up of vortex sheets. *Proc. R. Soc. Lond.* **A373**, 67

[34] Yang, Y. 1992 The initial value problem of a rising bubble in a two–dimensional vertical channel. *Phys. Fluids A* **4**, 913–920.

Figure Captions

Figure 1 Motion of the 2-D Boussinesq bubble. Solution of equations (6), (7) using a second–order Runge–Kutta method, $N = 128$, $dt = 0.001$ and a filter level of 10^{-13}. (a) The interface plotted at times $t = 0.0(0.1)1.6$ and $1.65(0.01)1.69$. (b) The sheet strength, γ, plotted against arclength for one half of the bubble. The sheet strength appears to form a cusp point at the critical time. (c) The curvature, C, of the interface plotted against arclength. At the critical time, the curvature seems to develop an infinite jump discontinuity.

Figure 2 The minimum radius of curvature of the sheet plotted against time for $N = 128, dt = 001$. Linear extrapolation from values for which the solution is known to be accurate and reliable gives an estimate for the critical time.

Figure 3 (a) Minimum radius of curvature against time for $N = 128$. $\square$: $dt = 0.01$; $\circ$: $dt = 0.005$; $\triangle$: $dt = 0.001$. (b) Minimum radius of curvature against time for $dt = 0.001$. $\square$: $N = 64$; $\circ$: $N = 128$; $\triangle$: $N = 256$.

Figure 4 (a) The Fourier coefficients of $z(\xi, t)$ plotted against wavenumber k, for the case $N = 256$, $dt = 0.001$, 13–digit arithmetic and a filter level of 10^{-13}. The time levels are $t = 0.0\,(0.1)\,1.6$ and $1.670\,(0.005)\,1.695$. The critical time is $t_c \approx 1.692$. (b) The Fourier coefficients of $z(\xi, t)$ plotted against $\log_{10} k$ for the same parameter values. A straight line envelope to the high wavenumber coefficients in the final spectrum indicates algebraic decay and the presence of a singularity.

Figure 5 (a) The algebraic decay $\mu(k)+1$ of the Fourier coefficients at $t = 1.65$ using $N = 128$, $dt = 0.001$, 13–digit arithmetic and a filter level of 10^{-13}. μ is taken to be *real.* No significance can be attached to any particular value of μ. (b) The algebraic decay $\Re(\mu(k) + 1)$ of the Fourier coefficients assuming μ is *complex* for the same parameter values. Although the scatter is eliminated there is no consistency in $\Re(\mu(k) + 1)$ as a function of k.

Figure 6 The algebraic decay $\Re(\mu(k) + 1)$ of the Fourier coefficients for $N = 128$, $dt = 0.001$, 28–digit arithmetic and a filter level of 10^{-28}. μ is taken to be complex. Results for (a) $k > 0$ and (b) $k < 0$. Particularly for $k < 0$, the value of $\Re(\mu(k)) + 1$ is consistently close to 2.5 for $|k| \leq N/2$. The deterioration for $k \geq N/2$ arises because (13) was derived for infinite Fourier series.

Figure 7 The exponential decay $\delta(k)$ of the Fourier coefficients plotted as a function of k for the case $N = 128$, $dt = 0.001$, 28–digit arithmetic and a filter level of 10^{-28}. From the top of the figure the times are $\circ$: 1.61; $\times$: 1.62; $*$: 1.63; $+$: 1.64; $\circ$: 1.65; $\times$,: 1.66; $*$: 1.67; $+$: 1.68; $\circ$: 1.69; $\times$: 1.70. The coefficients for $k < 0$ yield more consistent values of δ at each time than those for $k > 0$. Clearly $\delta(k)$ decreases to zero at a finite time.

Figure 8 The effect of the filter level on $\Re(\mu(k) + 1)$ at $t = 1.65$ for $N = 128$, $dt = 0.001$ and 28–digit arithmetic. Filter level $\square$: 10^{-14}; $\circ$: 10^{-15}; $\triangle$: 10^{-16}; $+$: 10^{-17}; $\times$: 10^{-18}.

Figure 9 The effect of increasing the number of points (and therefore modes) on the accuracy of fitting to the Fourier coefficients. As N is doubled the number of coefficients giving consistent values of $\Re(\mu+1)$ is approximately doubled. The plot is for the extrapolated critical time $t_c^\infty = 1.689$. Results for (*a*) $k > 0$ and (*b*) $k < 0$. $\square$: $N = 32$; $\circ$: $N = 64$; $\triangle$: $N = 128$; $+$: $N = 256$.

Figure 10 The algebraic decay against time for $t = 1.65\,(0.005)\,1.70$ with $N = 128$, $dt = 0.001$ and using the $k < 0$ coefficients. The mean value of $\Re(\mu)$ slowly increases as $t \longrightarrow t_c$.

Table Captions

Table 1 The estimated critical times, t_c, obtained from plots of (maximum curvature)$^{-1}$ versus time. Filtering was applied after each time step. Too much filtering leads to the increase in the critical time illustrated by the value in the final column.

Table 2 The times, τ, at which the Krasny filtering technique is switched off for the interfacial position z and the vortex strength V. The values in italics come from the expressions $\tau = 1.70 - 7.36\,N^{-1}$ for z, and $\tau = 1.70 - 2.50\,N^{-1}$ for V.

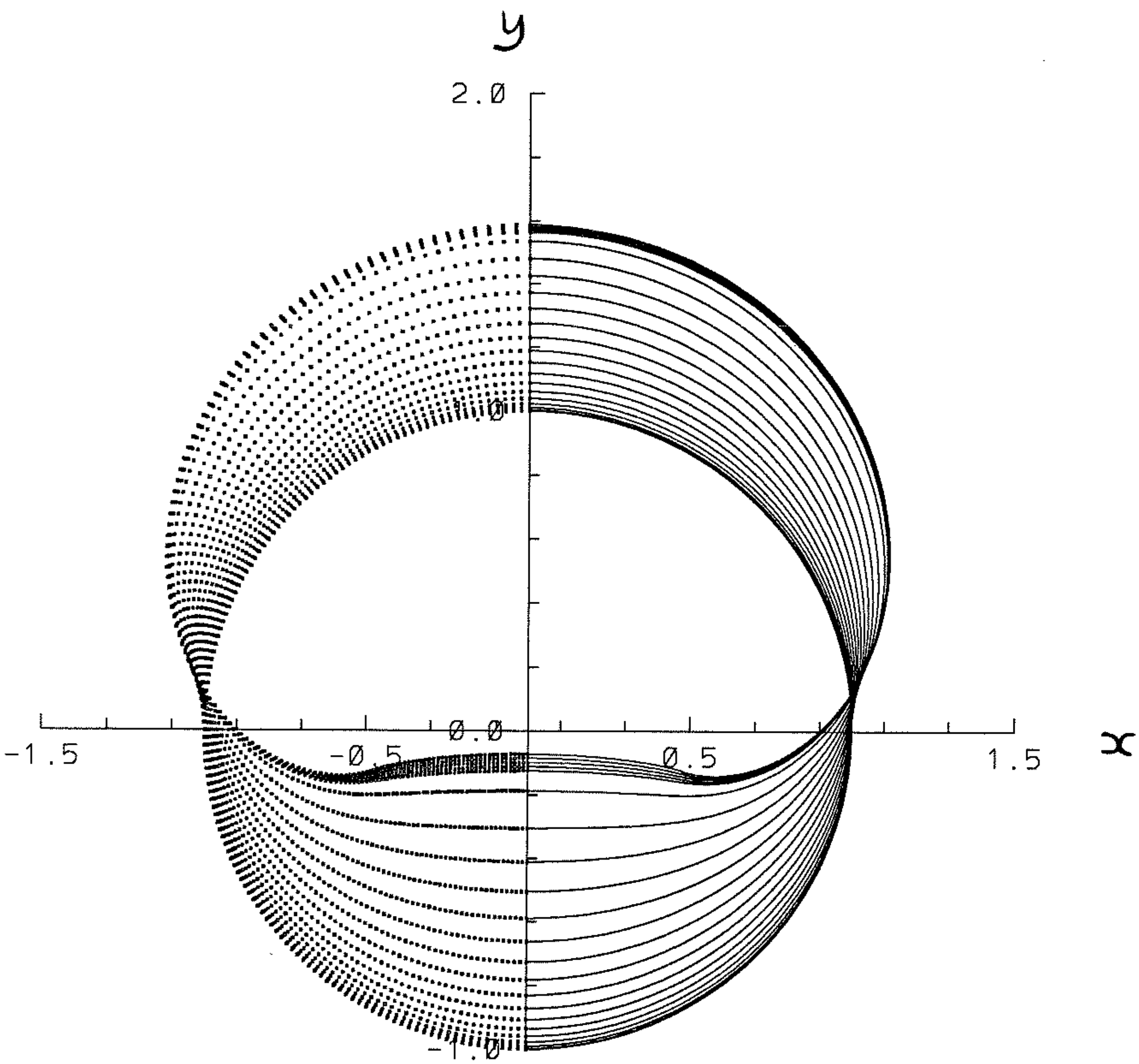

Figure 1(a)

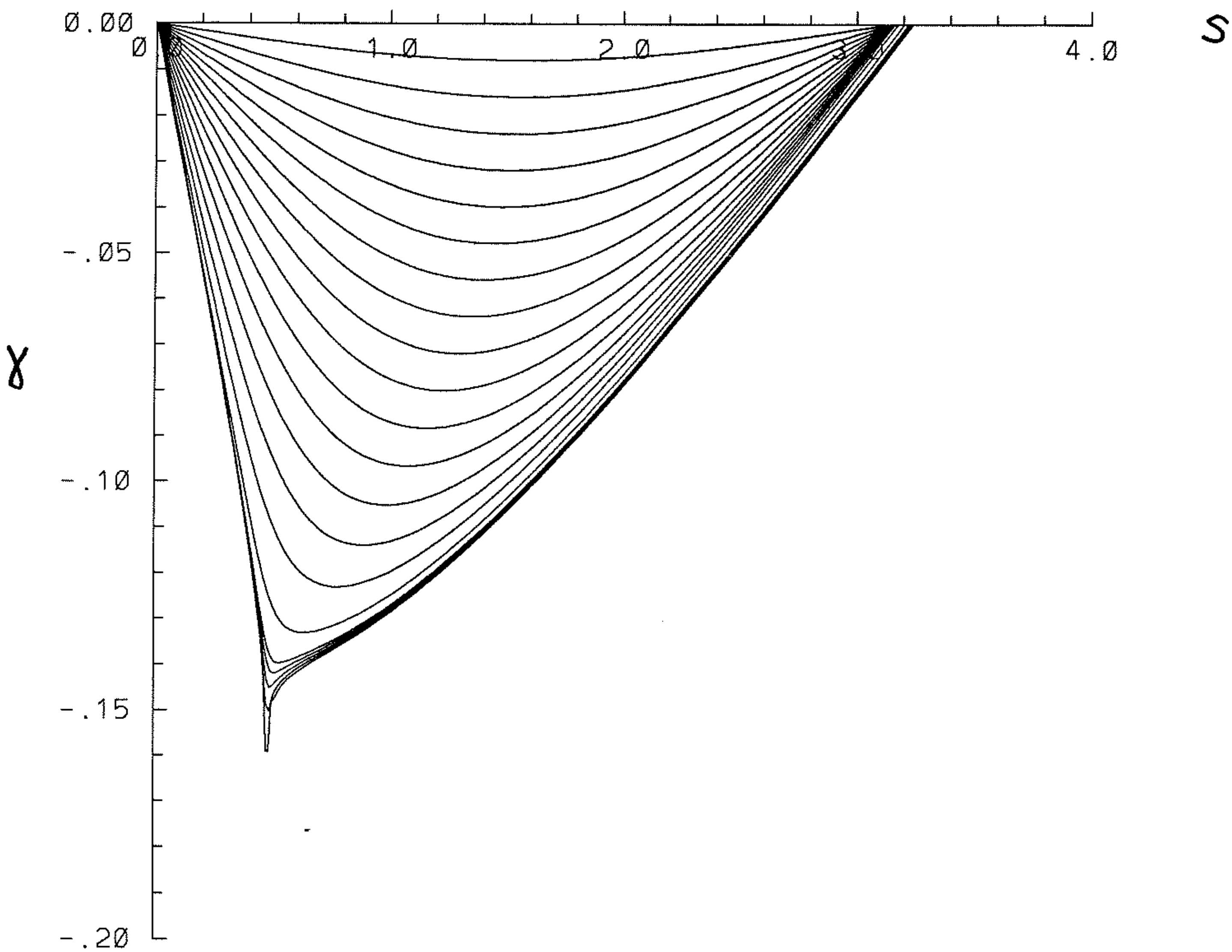

Figure 1(b)

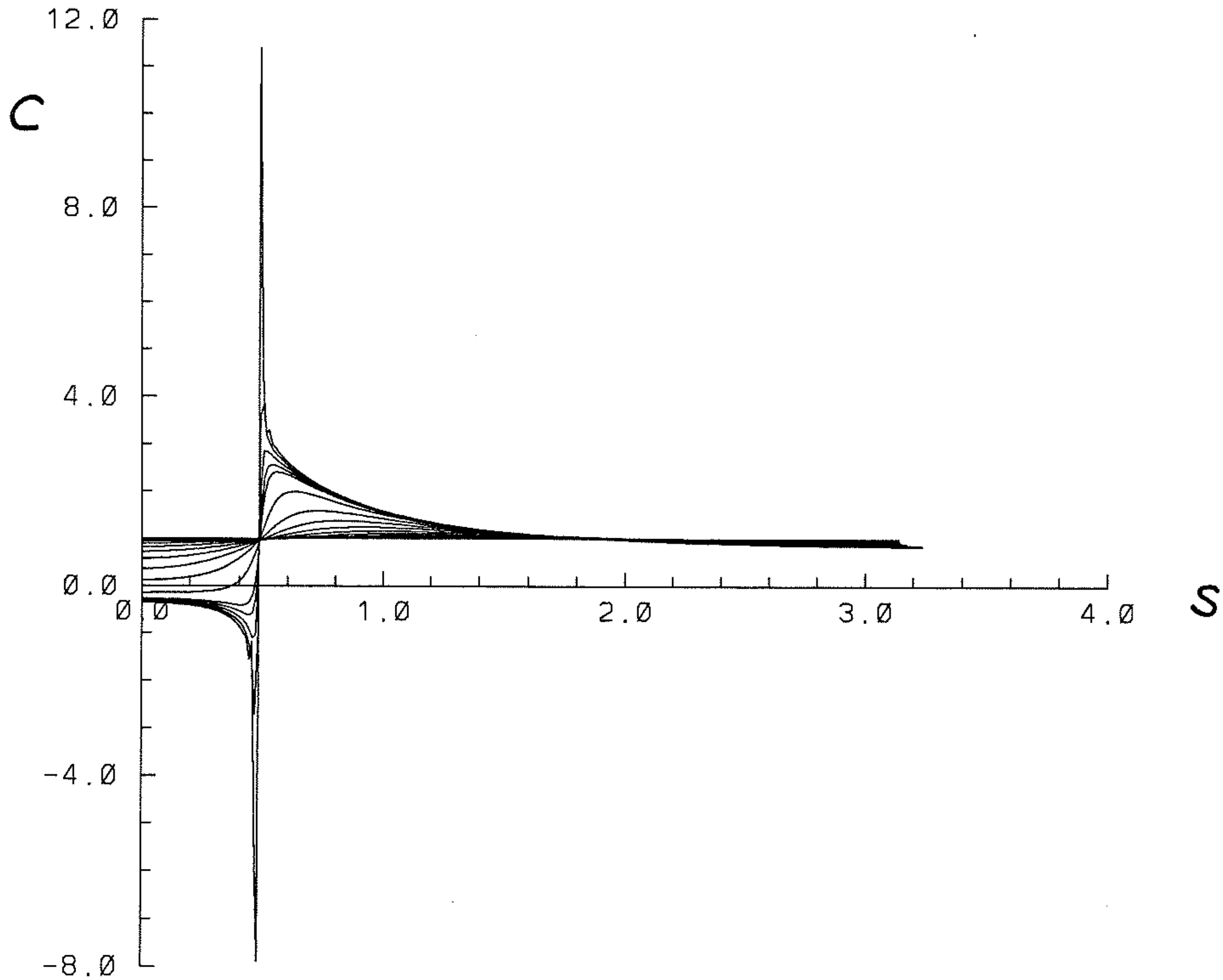

Figure 1(c)

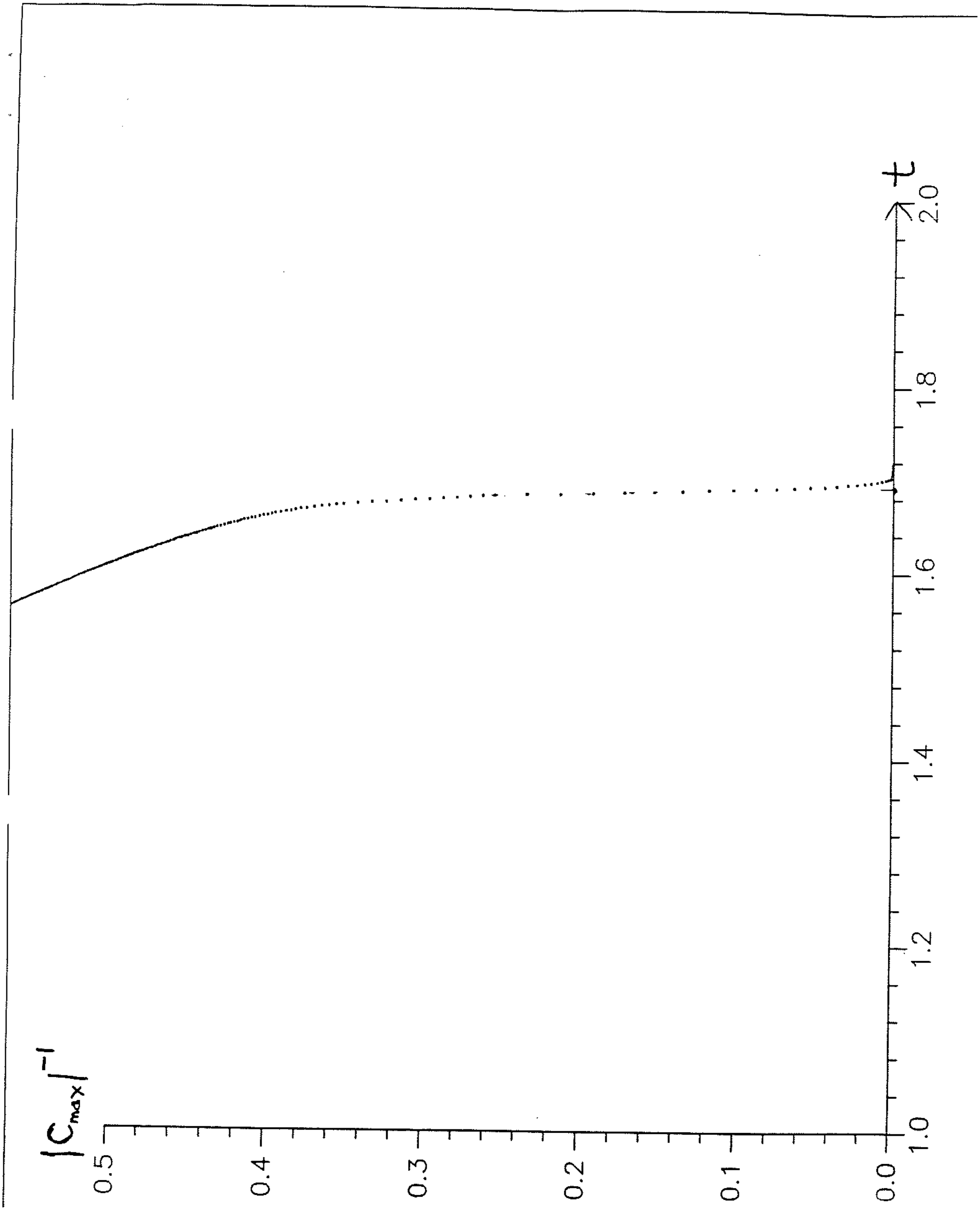

(Maximum curvature)$^{-1}$ against t (time) for N = 128, dt = 0.001.

fig. 2

(a) The radius of curvature clearly tends towards zero. Linear extrapolation from values for which the solution is known to be accurate and reliable, gives an estimate of the

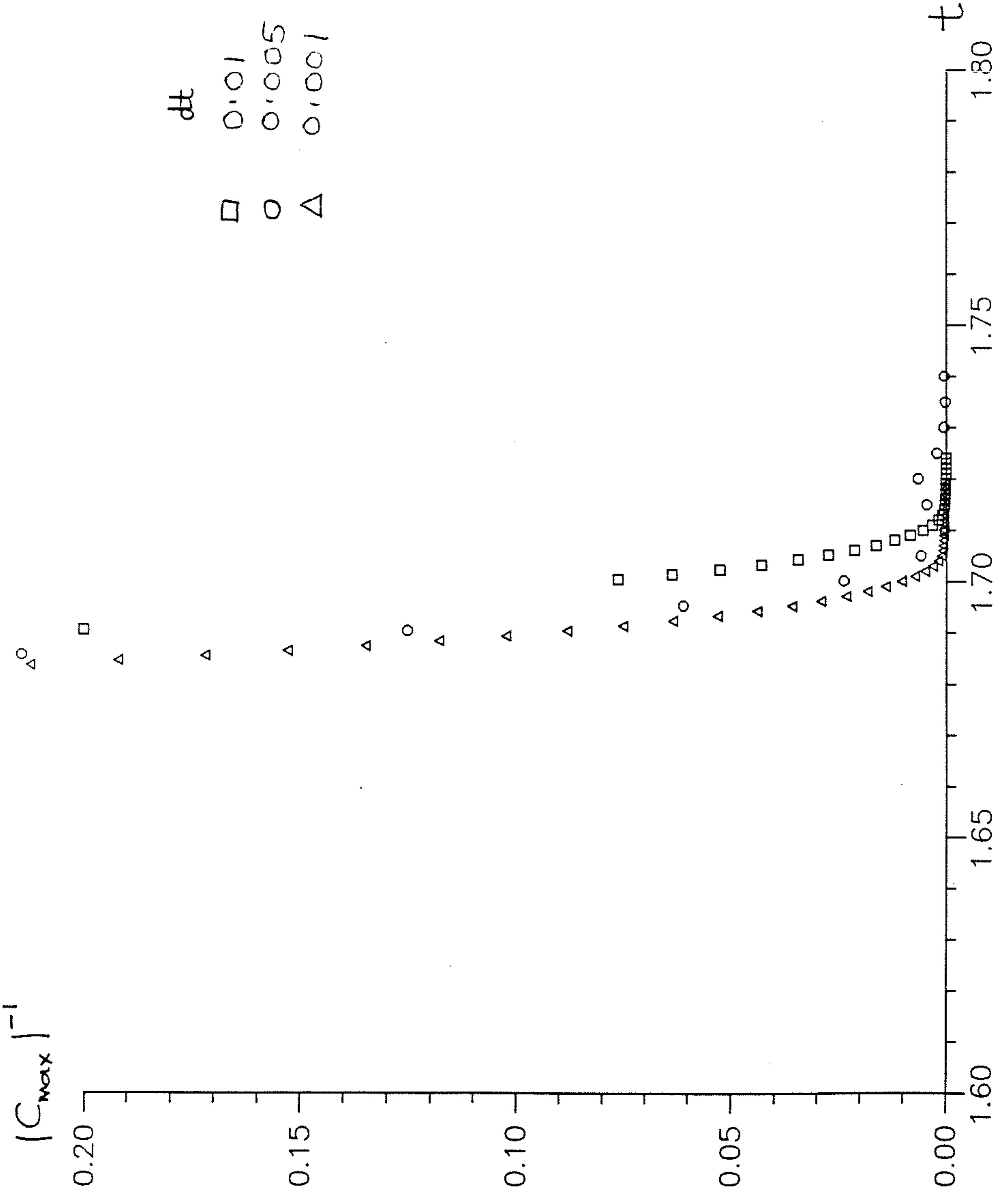

Figure 3(a) $(C_{max})^{-1}$ against t for N = 128 and dt = 0.01, 0.005, 0.001 demonstrating the convergence as dt $\longrightarrow$ 0 for fixed N.

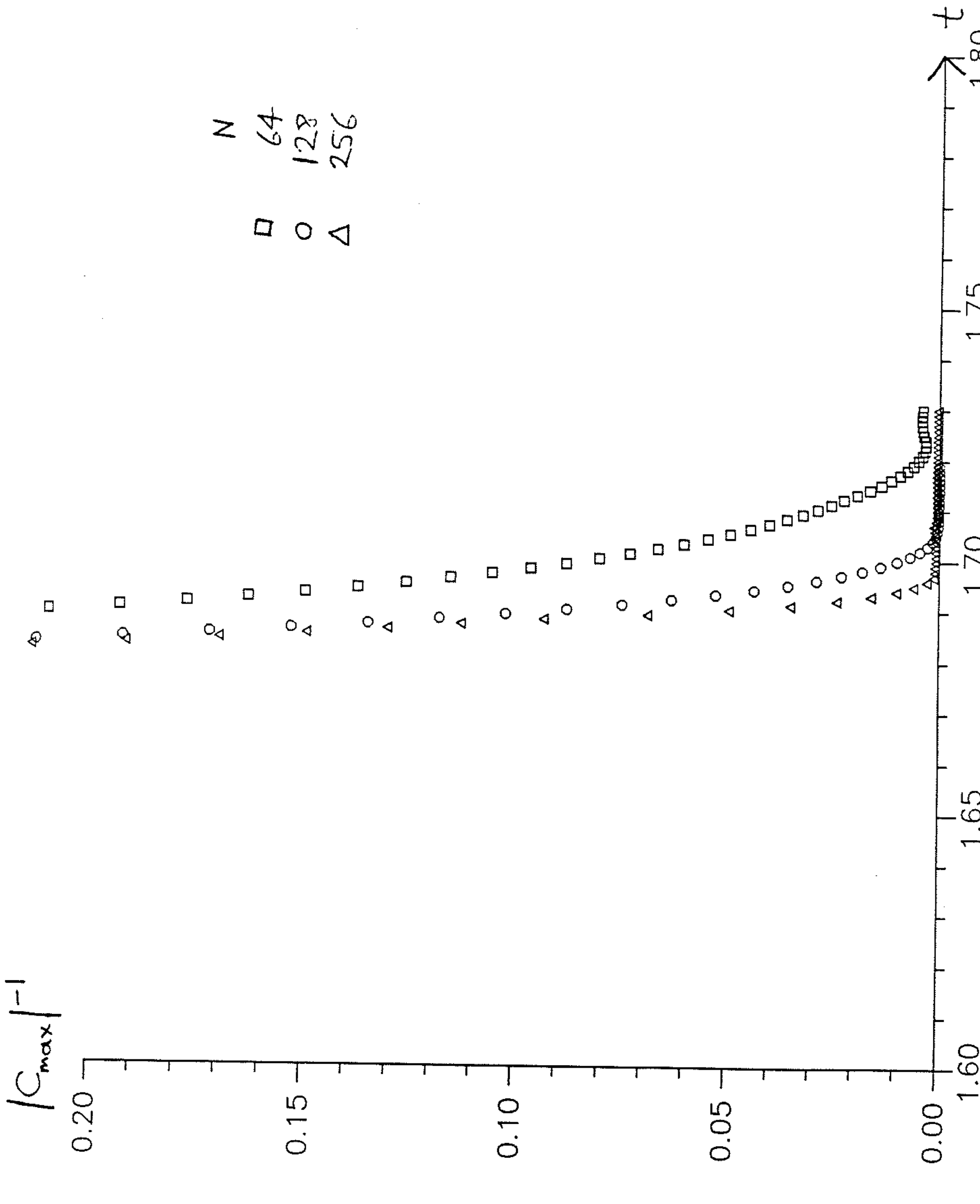

Figure 3(b) $(C_{max})^{-1}$ against t for dt = 0.001 and N = 64, 128, 256 demonstrating convergence as N $\longrightarrow \infty$ for fixed dt.

263 Figure 4(a)

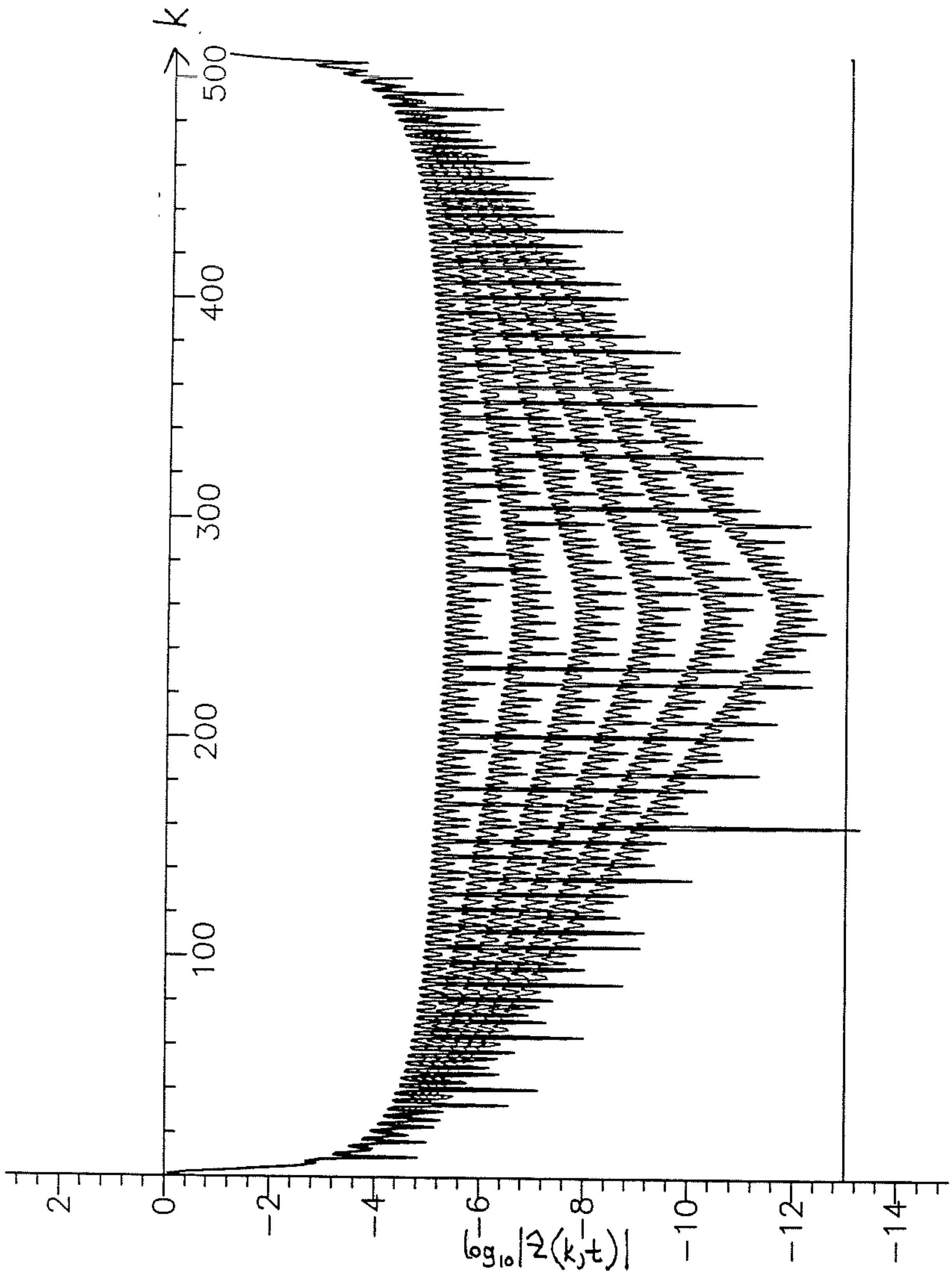

~~Figure 3(a)~~ Solution in Fourier space using N = 256, dt = 0.001 in 13 digit arithmetic with filter level 10^{-13}. The singularity time for this solution is 1.692.

(a) Plot of $\log_{10}|\hat{z}(k,t)|$ against k (wavenumber) at t =

Fig. 4(b)

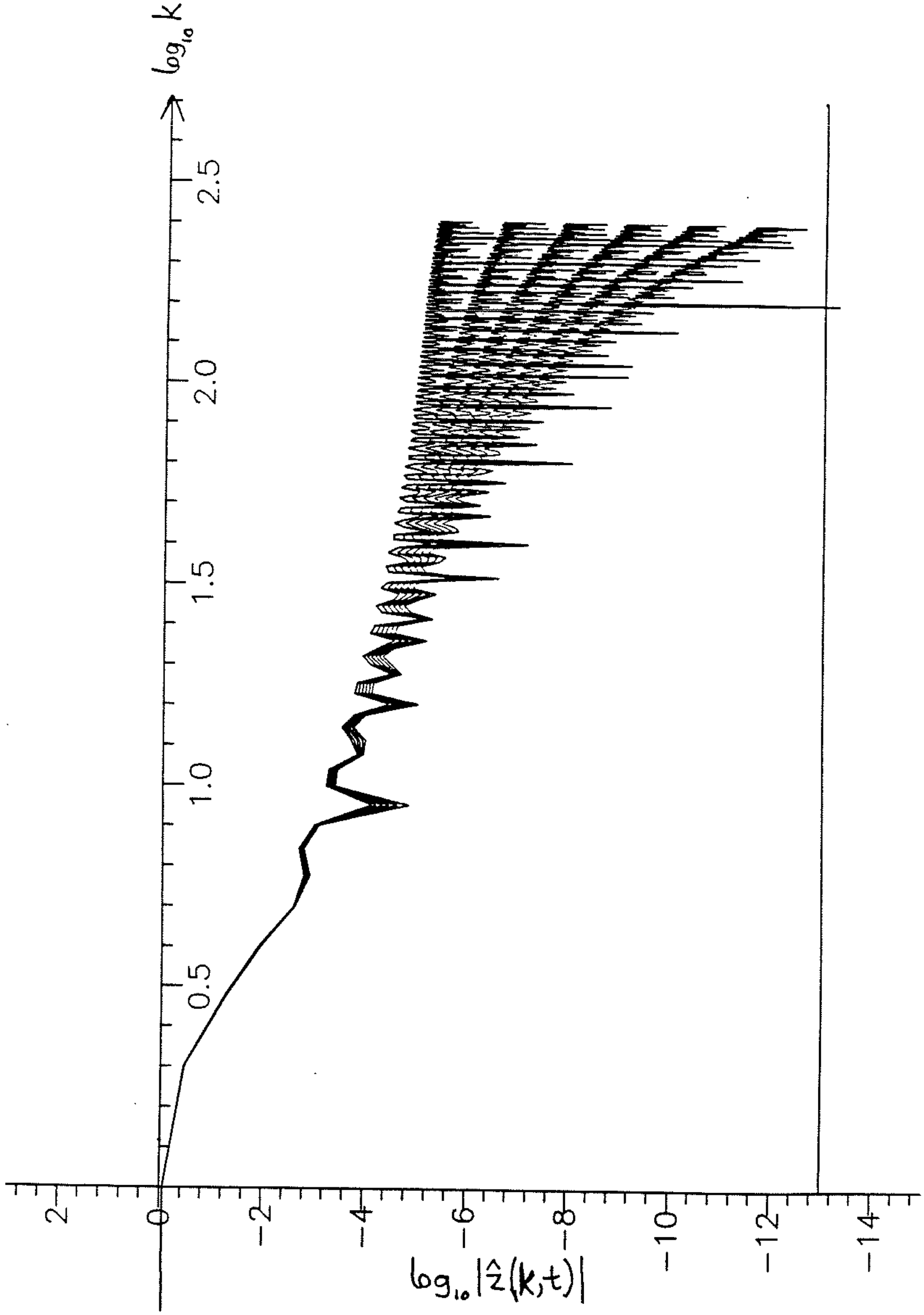

(b) $\log_{10}|\hat{z}(k,t)|$ against $\log_{10}k$. The straight line envelope to the high wavenumber coefficients in the final spectrum ($t = 1.695$) indicates algebraic decay and a singularity has developed.

Fig. 5(a)

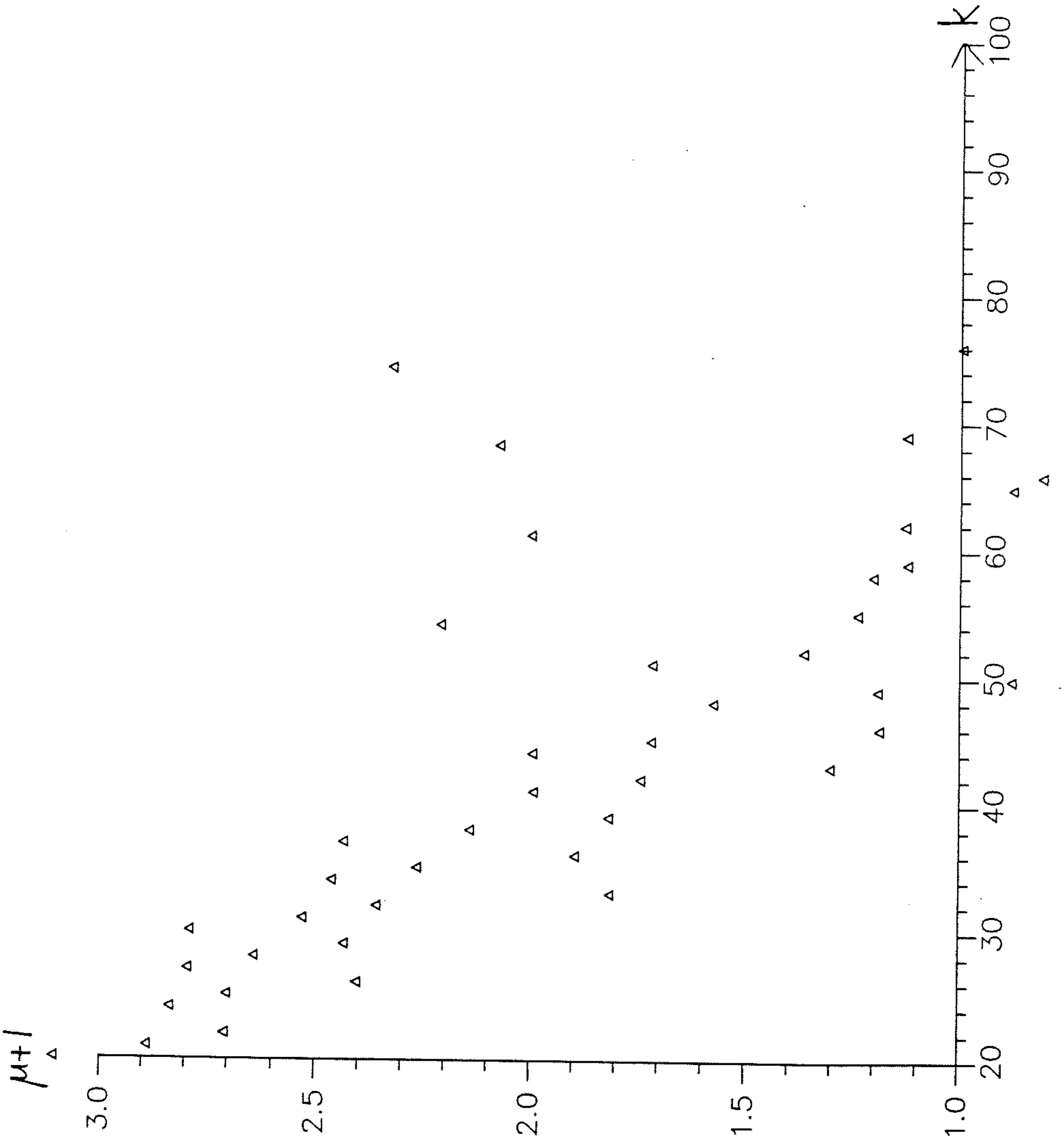

~~Figure 3.11~~ Algebraic decay, $\mu+1$, of Fourier coefficients at t = 1.65 using N = 128, dt = 0.001, 13 digit arithmetic, filter level 10^{-13}.

~~Figure 5~~

(a) The values $\mu(k) + 1$ were obtained from expression (3.7.4) centred about each value of k assuming μ was entirely *real*. No significance can be attached to any particular

273 Fig. 5(b)

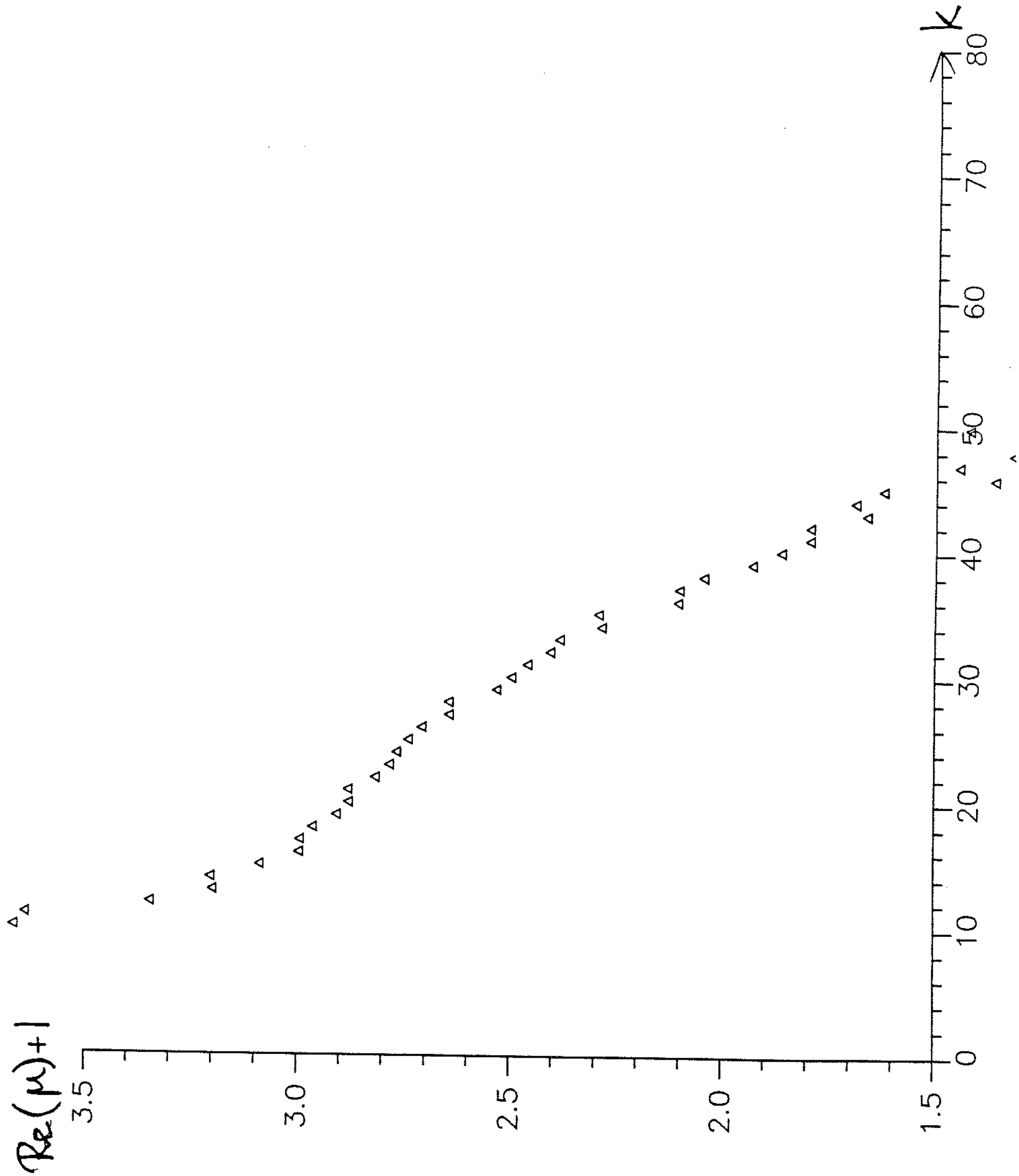

Same as (a) except that μ is *complex*. The algebraic decay is given by $\mathbb{R}\mathrm{e}(\mu)+1$. The scattering in (a) is removed and the values decrease monotonically.

Fig. 6 (a)

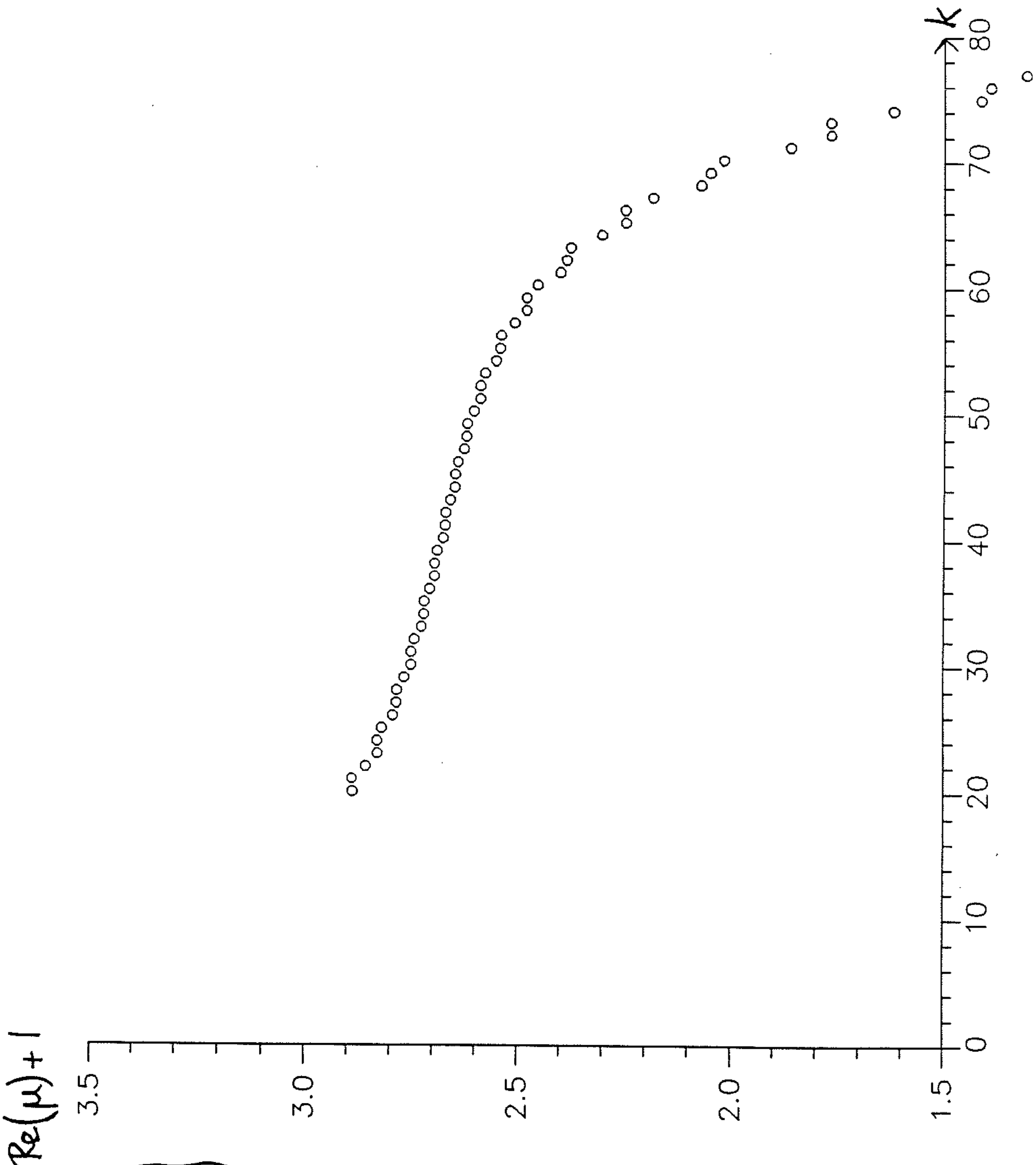

Algebraic decay of Fourier coefficients at $t = 1.65$ using $N = 128$, $dt = 0.001$ when computations are performed using 32 digits and filter level 10^{-32}. μ is complex.

(a) $\mathbb{R}e(\mu) + 1$ against k ($k > 0$)

Fig 6(b) 275

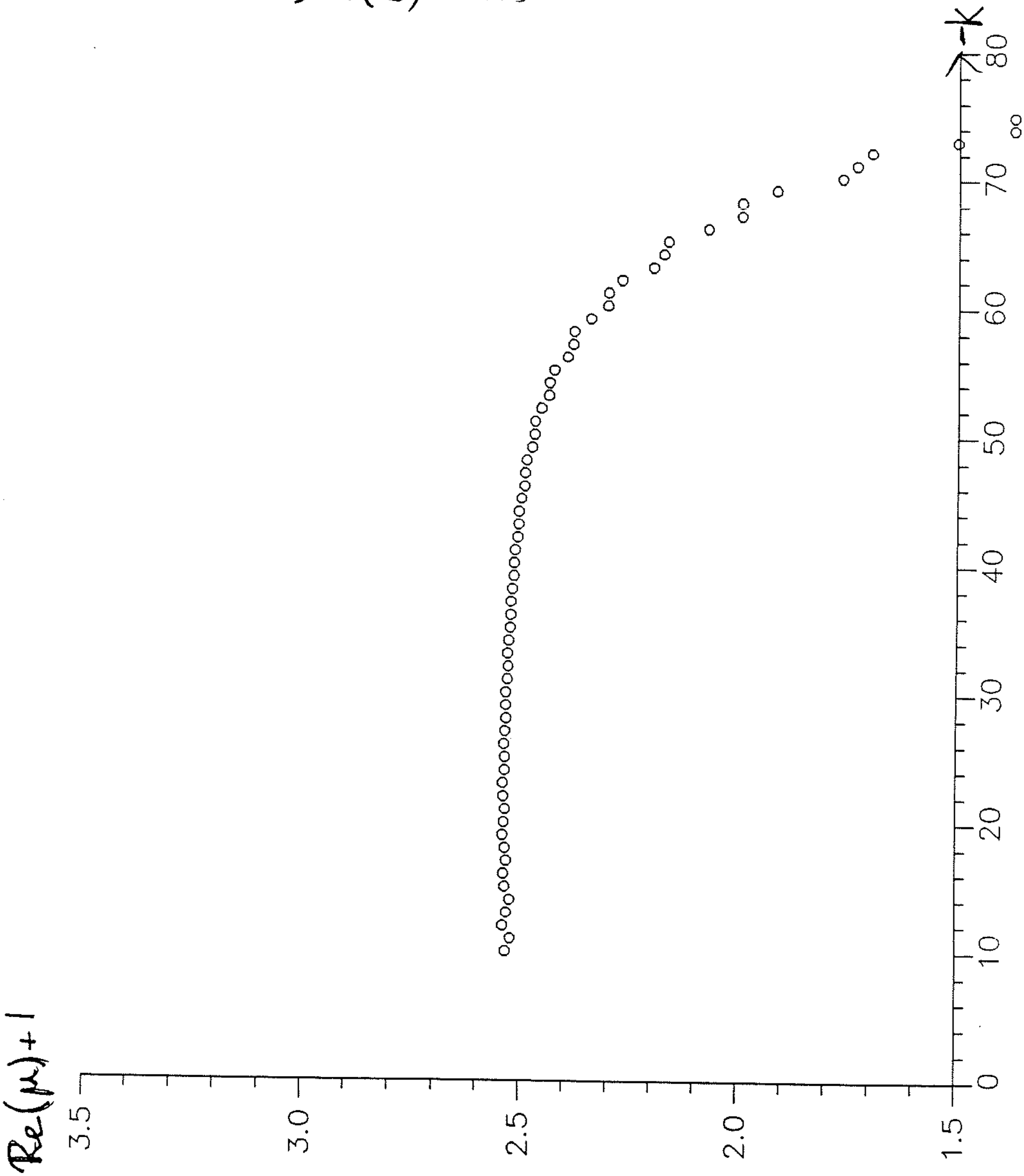

Re(μ) + 1 against k (k < 0)
The value is consistently 2.5 for $-k \leq N/2$; the deterioration of Re(μ)+1 for $k > N/2$ arises from errors in calculating the high wavenumber Fourier coefficients and the ill conditioned nature of the equations for Re(μ)+1.

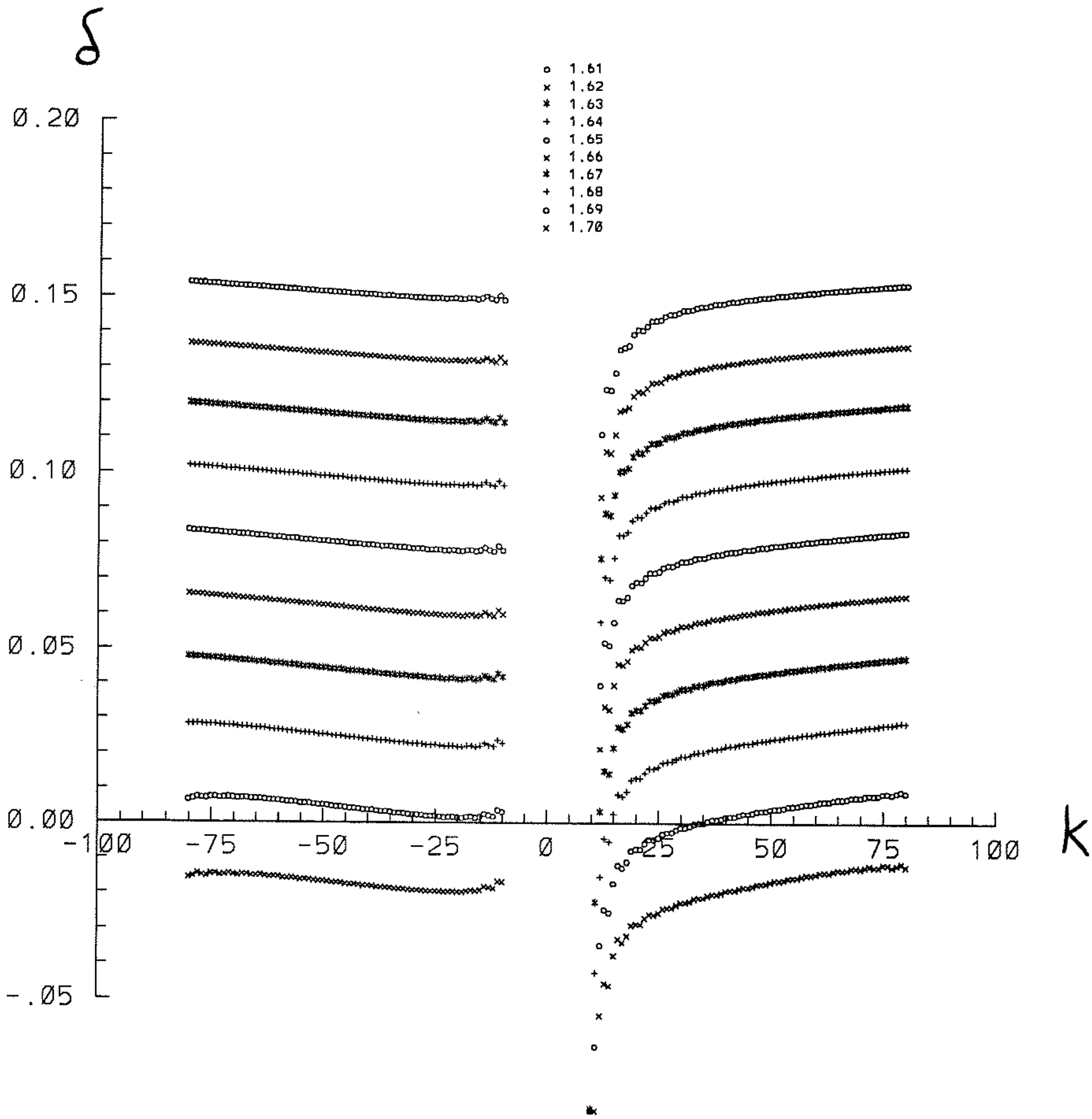
δ
o 1.61
x 1.62
* 1.63
+ 1.64
o 1.65
x 1.66
* 1.67
+ 1.68
o 1.69
x 1.70
Ø.2Ø
Ø.15
Ø.1Ø
Ø.Ø5
Ø.ØØ
-.Ø5
-1ØØ
-75
-5Ø
-25
Ø
25
5Ø
75
1ØØ
K

Figure 7

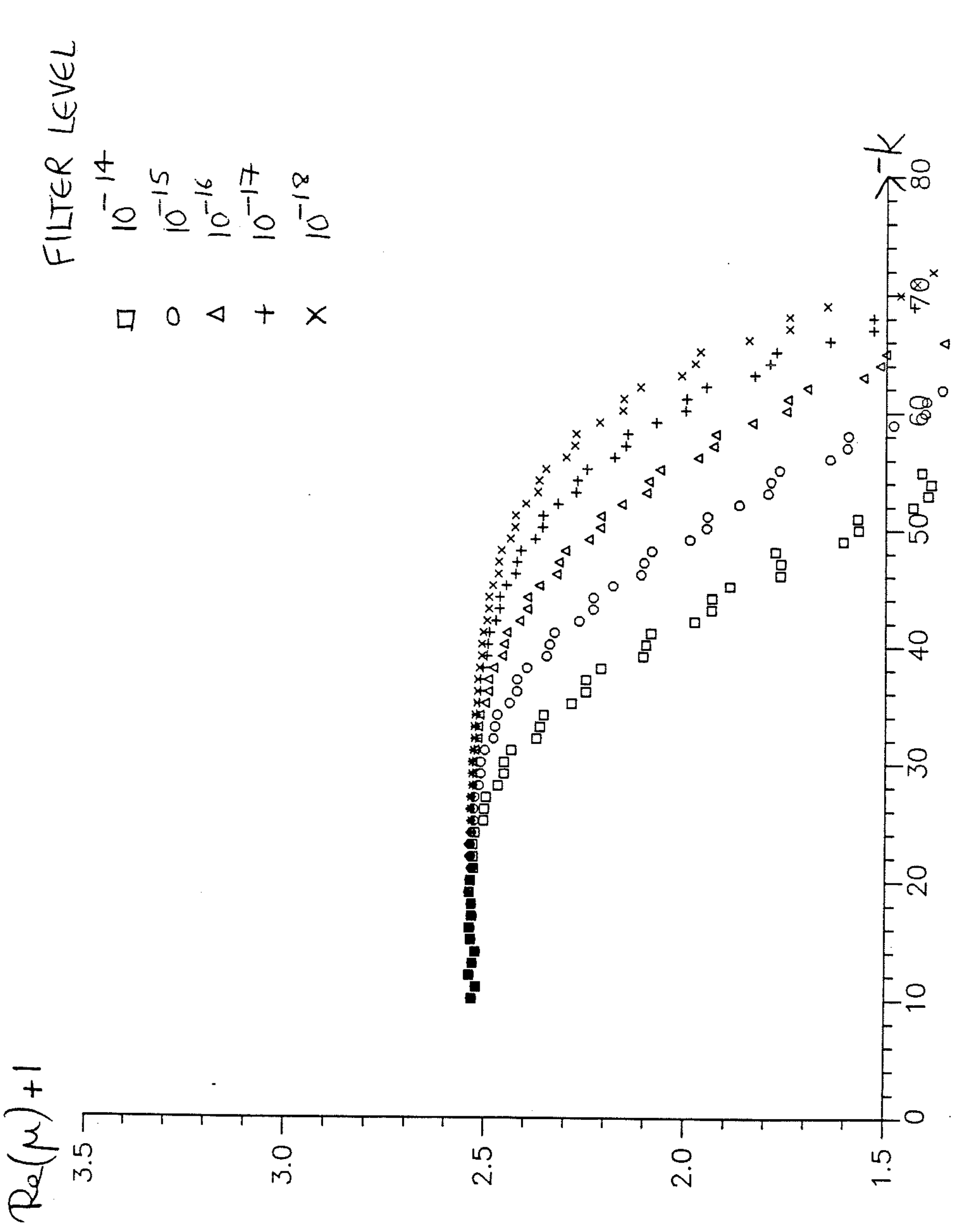

~~Figure 2.13~~ Figure 18 The effect of the filter level on $Re(\mu)+1$ at $t = 1.65$ with $N = 128$, $dt = 0.001$ using 32 digit arithmetic. The filter level varies from 10^{-13} to 10^{-18}. The deterioration is clearly evident as the filter level is increased.

Fig. 9 (a) 279

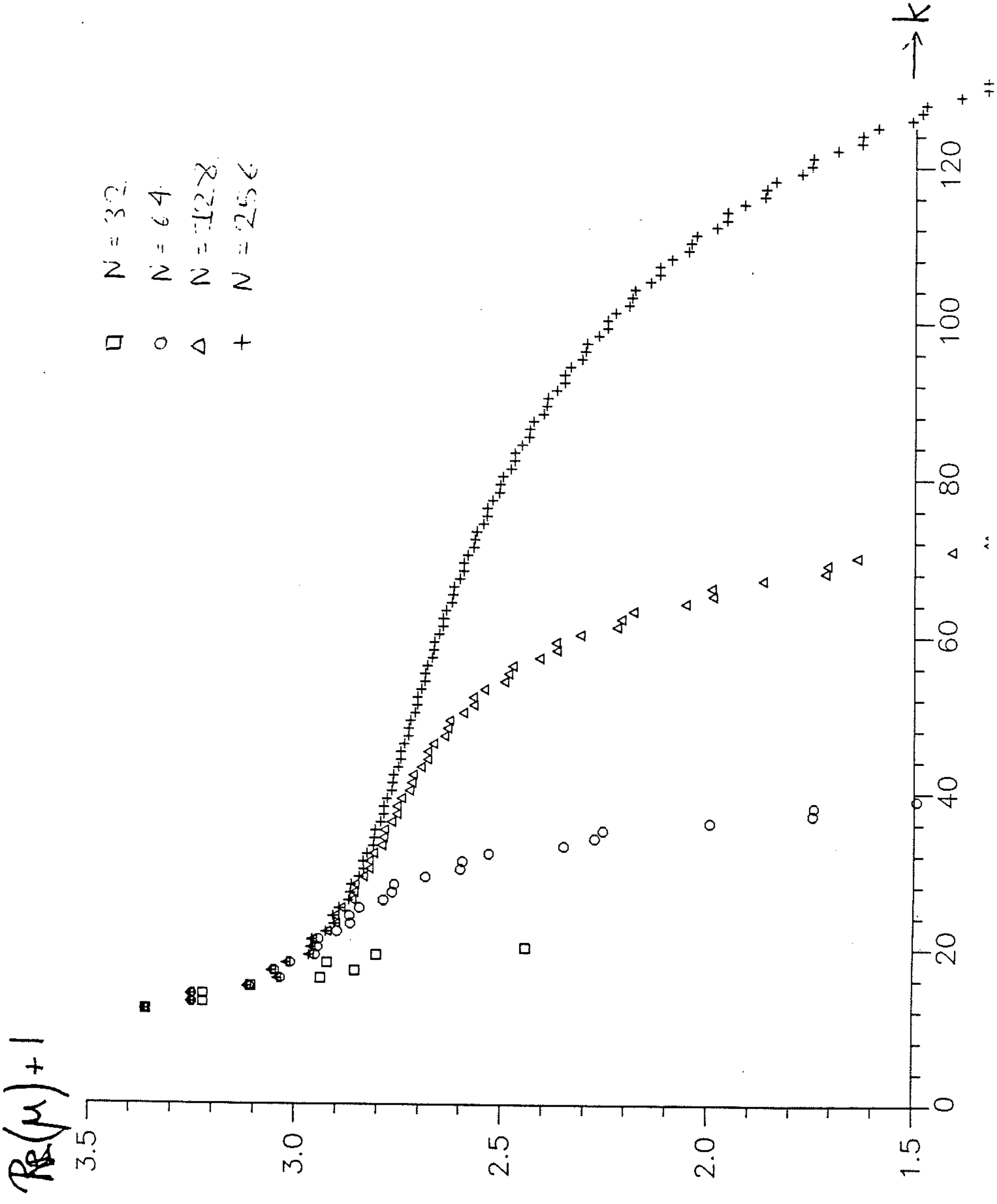

Effect of increasing the number of points (and therefore modes) on accuracy of Fourier coefficients. As N is doubled the number of coefficients giving consistent values of $\mathrm{Re}(\mu)+1$ is approximately doubled. The time level is the extrapolated critical time $t_c^{\infty} = 1.689$.

Fig 9(b)

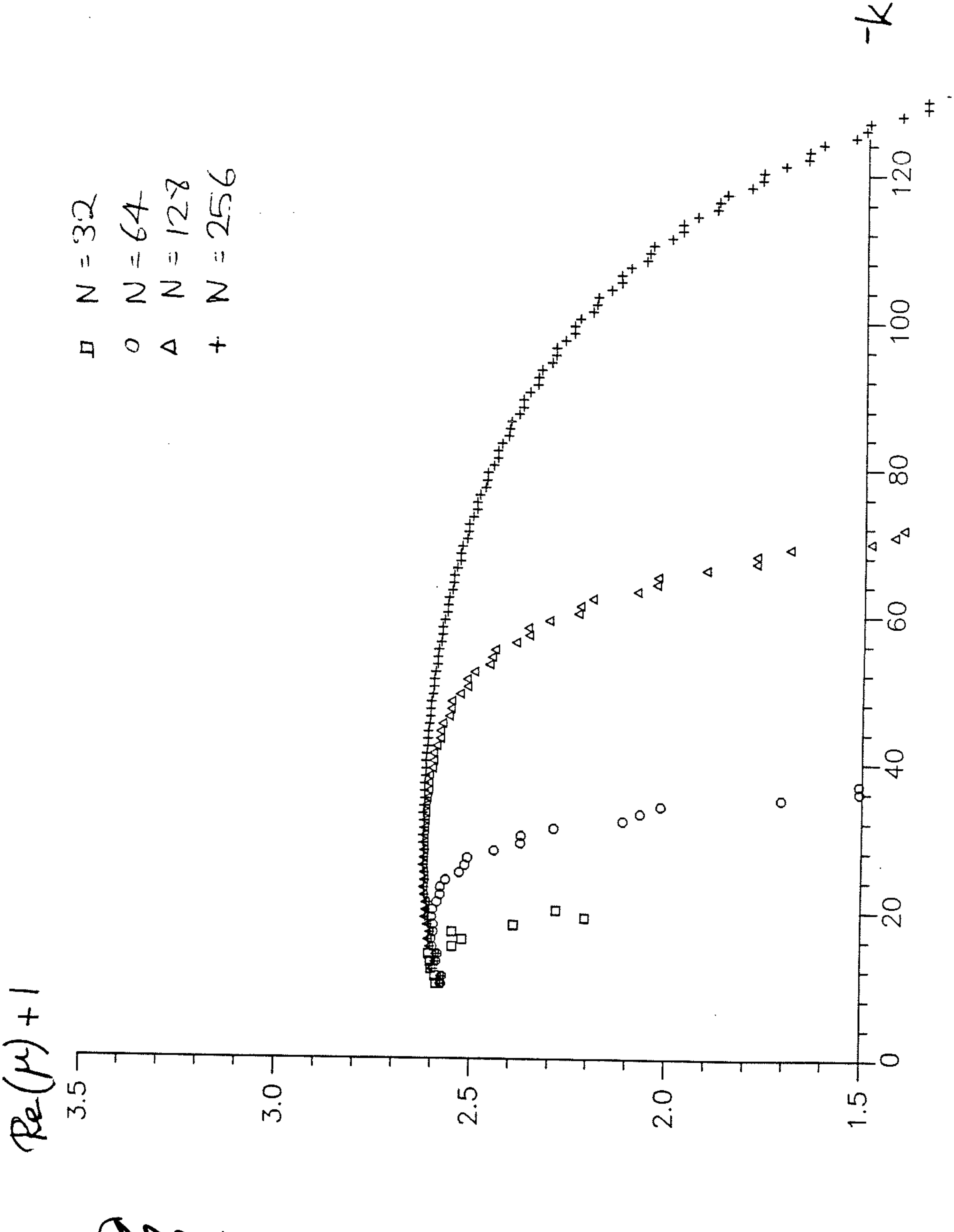

k < 0

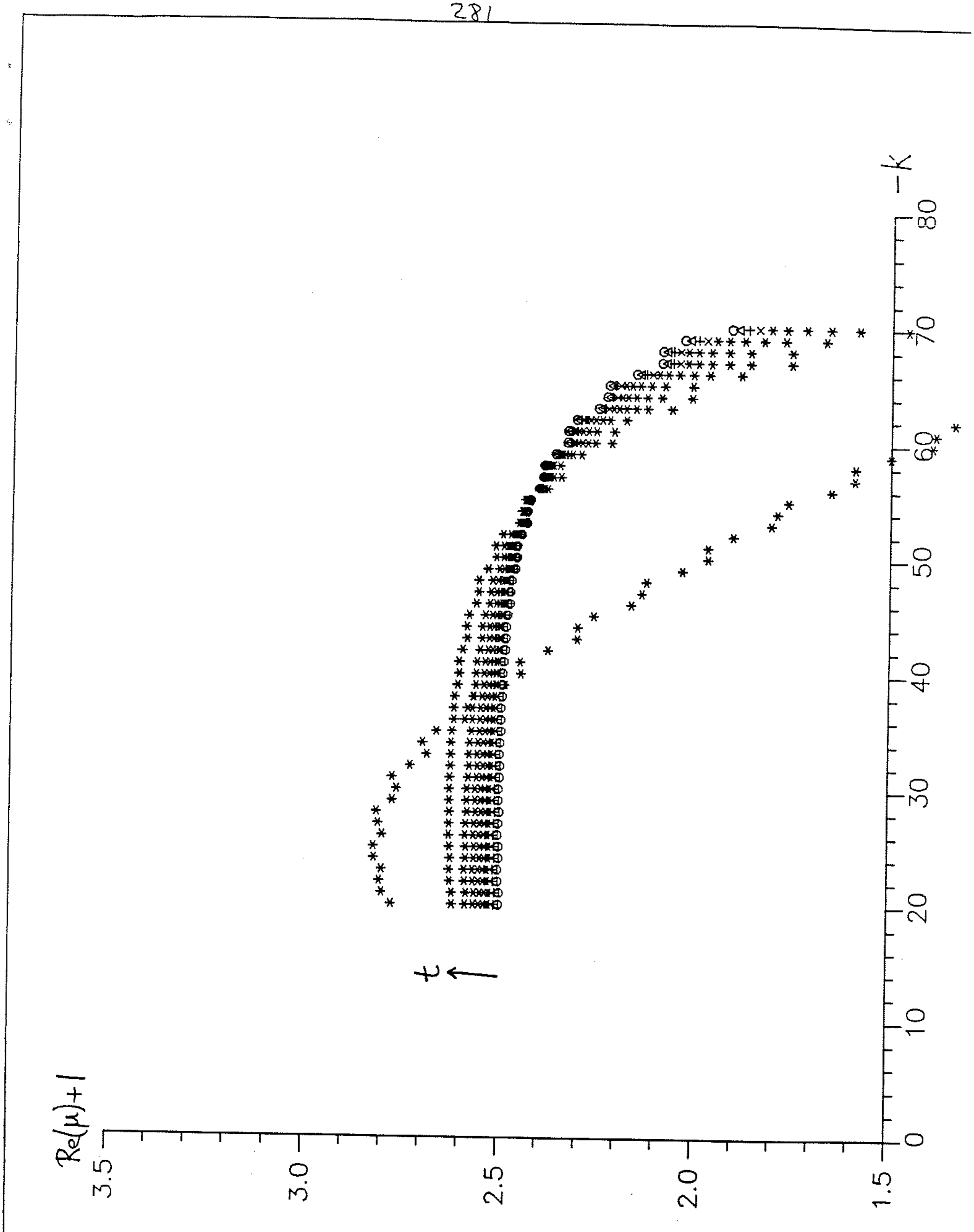

~~Figure 3.10~~ Re(μ)+1 versus k at t = 1.65 (0.005) 1.70 using N = 128, dt = 10^{-3}.

Figure 10

The 'average' value of Re(μ)+1 increases as t approaches the critical time.

N \ dt	0.01	0.005	0.001	0.0001
64	1.717	1.710	→ 1.702	
128	1.707	1.697	→ 1.695	1.705
256	1.706	1.697	→ 1.692	

Table 1 ~~Table 3.5~~ The estimated critical times t_c obtained from plots of (maximum curvature)$^{-1}$ vs time for the two dimensional Boussinesq bubble. Filtering was applied after each time step. Too much filtering delays the critical time as demonstrated by the value in the final column.

An expression of the form $t_c^N = t_c^\infty - \frac{\alpha}{N}$ was fitted to the arrowed values using linear least squares giving $t_c^\infty = 1.689$ and $\alpha = 0.771$.

$z(\xi)$

dt / N	0.01	0.005	0.001	0.0001
32	1.36	1.365	1.393	
64	1.57	1.565	→ 1.585 *1.585*	
128	1.65	1.645	→ 1.643 *1.6425*	1.6560
256	1.69	1.675	→ 1.671 *1.67125*	

$V(\xi)$

dt / N	0.01	0.005	0.001	0.0001
32	1.51	1.510	1.539	
64	1.65	1.650	→ 1.657 *1.661*	
128	1.69	1.680	→ 1.682 *1.680*	1.6937
256	1.72	1.700	→ 1.691 *1.690*	

Table 2 ~~Table 3.6~~ The times, τ, at which the Krasny filtering technique is switched off (when all the modes have grown above the filter level of 10^{-13}) for interfacial position $z(\xi)$ and point vortex strength $V(\xi)$. The values in italics come from the expressions $\tau = 1.70 - \frac{7.36}{N}$ for $z(\xi)$ and $\tau = 1.70 - \frac{2.50}{N}$ for $V(\xi)$; the coefficients were obtained by fitting expressions of the form $\tau = \alpha - \frac{\beta}{N}$ to the values which are arrowed.